1



Current Indian Science

Content list available at: https://currentindianscience.com



REVIEW ARTICLE

Recent Developments of Nanostructured Photocatalysts Based on Semiconducting Chalcogenides for Organic Reactions

Ramani Hazarika¹, Deepshikha Roy¹, Deepshikha Das¹ and Kalyanjyoti Deori^{1,*}

Abstract:

The earth-abundant metal chalcogenide is a highly versatile semiconductor with unique electronic and optical properties that seem to outperform the photocatalytic properties of metal oxides and metal nanoparticles. For ages, researchers are reaping the benefits of its photocatalytic properties in numerous reactions. However, the high charge recombination rates, poor compositional stability, and a smaller number of catalytically active sites restrict its application. The development of different kinds of heterojunctions by the combination of metal-chalcogenides with other conducting and semiconducting materials like metal oxides, metal nanoparticles, $g-C_3N_4$, single-atom catalysts, and MOF results in superior photocatalytic activity. This review provides insight into the various classes of metal-chalcogenide-based heterostructures and their application in various organic transformations. A brief overview of the synergistic properties arising from the development of such heterostructures helps to understand the surface interactions so that highly stable, efficient, and selective metal-chalcogenide-based heterostructures can be developed for industrially important photocatalytic organic transformations. This review also describes the role of mediators in boosting the stability and catalytic efficiency of the metal chalcogenides. Moreover, a thorough emphasis on the morphological impact of photocatalysts in various reactions will help with the development of metal chalcogenide heterostructures with tunable morphology and bandgap.

Keywords: Nanostructured, Photocatalysts, Semiconducting, Chalcogenides, Organic reactions, Heterostructures.

Article History Received: February 20, 2024 Revised: April 10, 2024 Accepted: April 16, 2024

1. INTRODUCTION

The ever-escalating global energy consumption is leading the world towards sustainable development. Solar energy serves as an indomitable renewable energy resource for driving numerous catalytic processes. The earth-abundant metal chalcogenides such as CdS, CdSe, MoSe₂, Bi₂S₃, and CuS serve as an excellent class of semiconductor photocatalytic material because of their unique electronic properties and narrow optical bandgap (1-3 eV). Their low toxicity, bio-compatibility, abundant surface-active sites, and tunable redox potential are also some other prominent properties resulting in their increasing popularity [1 - 3]. However, the high charge recombination rates, poor compositional stability, and a smaller number of catalytically active sites result in a challenge when using them as a photocatalyst [4]. The emergence of metalchalcogenide-based heterostructures with other semiconducting and conducting materials such as metal oxides (CdS/TiO₂ [4], CdS/ZnO [5], CeO₂/CdS [6], TiO₂/MoS₂ [7]), metal nanoparticles (Ni/CdS [8], Co/CdS [9], Cu/CdS [10], Pd/CdS [11]) and new age materials such as g-C₃N₄ [12 - 18], single

atom catalyst [19] and MOF [20] puts forward a solution for the rapid charge recombination faced by metal-chalcogenides alone. Such heterostructures result in a variety of heterojunctions like Vanderwaal heterojunction, p-n junction, Schottky barrier, etc., which enhances the lifetime of the excitons, thus preventing rapid charge recombination and promoting superior photocatalytic activity. The hybridization of variable band gaps in such heterostructures gives rise to suitable band positions and better separation between the valence band (VB) and conduction band (CB), ultimately resulting in better electron transport [21 - 24]. It has been observed that morphology controlling various metal chalcogenides and their heterostructures induces an anisotropic effect, which results in high compositional stability along with the rise in highly exposed catalytically active sites and enhanced optical properties and charge separation [4, 21]. The core-shell structure of metal chalcogenides and their heterostructures consisting of a photoactive core and photosensitive shell prevents the surface dissociation of ions into the core, which provides them the much-required stability against photocorrosion [21, 25]. Other morphologies, such as 1D nanorods, lateral heterostructures, nanosheets, and dodecahedral morphologies of metal chalcogenide-based heterostructures also exhibit exquisite properties like quantum

¹Department of Chemistry, Dibrugarh University, Dibrugarh, India

^{*} Address correspondence to this author at the Department of Chemistry, Dibrugarh University, Dibrugarh, India; E-mails: kalchemdu@gmail.com and kalchemdu@dibru.ac.in

confinement effect, reduced charge recombination, controllable interfacial optoelectronic properties, and multiple reflections yielding better performance of metal chalcogenide-based heterostructures over their solo counterparts [26 - 29]. For a very long time, metal chalcogenides have been widely used for reactions such as the degradation of organic pollutants, dye degradation, reduction of Cr (VI), generation of solar fuel, and production of H₂ and O₂ by the photocatalysis of water [21, 30 - 33]. Conventional organic transformations usually require harsh reaction conditions like the use of toxic and corrosive oxidizing and reducing agents, as well as high temperature and pressure. So, recently, many researchers have shifted their attention towards using metal chalcogenides and their heterostructures as photocatalysts for organic transformations such as selective oxidation of sp³ saturated C-H bond of toluene and its derivative, oxidation of benzyl alcohol into aldehyde, oxidation of nitro aromatic to imines and many more under mild reaction conditions because of their narrow bandgap properties and versatile nature [34 - 36]. Keeping in view the limitations like low interfacial contact between the hybrids, poor catalytic sites, high charge recombination, and low amount of reactive center associated with the use of metal chalcogenides alone as a photocatalyst, this review puts emphasis on the synergistic properties arising from the development of new metal chalcogenide-based heterostructures with unmatched photocatalytic potentials. This review also discusses the morphological impact of metal chalcogenides and their heterostructures on reaction kinetics so that a good understanding of the photocatalytic reaction mechanisms can help to develop highly efficient and selective photocatalysts for sustainable organic transformations.

2. CHALCOGENIDE-BASED HETEROSTRUCTURES AND THEIR PHOTOCATALYTIC MECHANISMS IN VARIOUS ORGANIC REACTIONS

2.1. Chalcogenide-Metal Oxide Nanocomposites

Metal chalcogenide and metal oxide integration can significantly impact the photocatalytic characteristics of the resulting composite materials. Although metal oxides and metal chalcogenides have demonstrated potential as photocatalysts, they frequently face challenges like rapid charge recombination or inadequate light absorption. In comparison to individual components, the combination of metal oxides and chalcogenides frequently produces synergistic effects that increase the photocatalytic performance. Herein, we have discussed the photocatalytic activity and possible mechanisms in various organic transformations catalyzed by metal chalcogenides and metal oxide nanocomposites [24, 37].

2.1.1. CdS/TiO₂

Titanium dioxide (TiO₂) exhibits considerable potential in various environmental uses because of its unique attributes compared to alternative materials, including non-toxicity, affordability, simple preparation techniques, exceptional resistance to acids, water insolubility, and remarkable hydrophilicity. TiO₂ has been extensively researched and utilized as a photocatalyst, known for its remarkable capabilities in capturing solar energy for diverse applications.

Its ability to initiate photochemical reactions upon exposure to light enables the breakdown of organic pollutants, making it crucial for environmental remediation processes. The photocatalytic activity of TiO2 arises from its capacity to generate electron-hole pairs by absorbing photons, leading to redox reactions on its surface. Additionally, TiO2 finds applications in solar cells, self-cleaning surfaces, and antibacterial coatings, underscoring its versatility and significance in advancing sustainable technologies. In addition to its well-known applications in environmental remediation, TiO2 photocatalysis has gained prominence in the field of organic synthesis. This versatile photocatalyst has been employed in various organic reactions. This use of TiO₂ in organic synthesis underscores its role not only in environmental solutions but also in advancing the principles of green and sustainable chemistry. The use of TiO₂ as a photocatalyst, while advantageous in many respects, comes with several inherent limitations. One limitation is the high bandgap of TiO2 at 3.2 eV, positioning it in the ultraviolet range of the visible light spectrum [38 - 41]. The integration of chalcogenides with TiO₂ effectively mitigates challenges related to its restricted visible light absorption and rapid electron-hole recombination. This synergistic approach enhances the photocatalytic performance of TiO₂ by expanding its light absorption range and reducing charge carrier recombination, resulting in improved efficiency across various applications [42 - 44]. The incorporation of CdS into TiO₂ represents a promising approach to optimize and extend the photocatalytic capabilities of TiO₂ in diverse applications, from environmental remediation to organic synthesis [45, 46]. Onedimensional CdS@TiO, core-shell nanocomposites (CSNs) were synthesized using the solvothermal method. Various characterization techniques, such as UV-vis diffuse reflectance spectra, X-ray diffraction, photoluminescence spectra, fieldemission scanning electron microscopy, and electron spin resonance spectroscopy, were employed to analyze the structure and properties of the nanocomposites. The results indicate the formation of a 1D core-shell structure with TiO₂ coating onto CdS nanowires. The photocatalytic activities of these nanocomposites were evaluated for alcohol oxidation (Scheme 1), showing enhanced conversion and yield compared to bare CdS NWs.

After 8 hours of visible-light exposure, 1D CdS@TiO₂ CSNs showed significantly higher benzyl alcohol and benzaldehyde conversion and yield (34% and 33%, respectively) compared to CdS NWs (13% conversion and 12% yield). This enhanced photoactivity extended to other alcohol substrates, such as p-nitro benzyl alcohol and p-fluoro benzyl alcohol. The improved photocatalytic performance of CdS@TiO₂ CSNs is attributed to prolonged charge carrier lifetime and efficient hole trapping by TiO₂, leading to a distinct reaction mechanism in alcohol oxidation under visible light [4].

The mesoporous CdS–sensitized TiO_2 NPs (CdS-MTA) were synthesized using a surfactant-assisted self-assembly method. The resulting photocatalyst exhibits a 3D interconnected network of anatase TiO_2 NPs and CdS quantum dots, providing a large surface area of about 157 m 2 g $^{-1}$ and

R=H, CI, F, NO₂, CH₃, OCH₃

Scheme (1). Photocatalytic alcohol oxidation using 1D CdS@TiO₂ CSNs.

R= H, OMe, Cl, Me, NO₂

Scheme (2). Photooxidation of para-substituted aromatic alcohol using Cd-MTA.

uniform pores with a size of 7 nm. The CdS-MTA photocatalyst was employed for the photooxidation of parasubstituted aromatic alcohol using molecular oxygen as the oxidant, leading to the formation of its corresponding product (Scheme 2).

During the reaction, it was apparent that all the benzyl alcohol got oxidized to form its corresponding carbonyl compound. Notably, the oxidized product of para-nitrobenzyl alcohol exhibited a lower yield compared to others, attributed to the electron-withdrawing property of the nitro (NO₂) group. In contrast, for the methoxy and methyl substituents at the para position, the yields were 100% and 72%, respectively. This difference can be rationalized by the ability of electron-donating groups to stabilize radical cations in the transition state, leading to a faster rate and higher yield [47].

2.1.2. CdS/ZnO

Zinc oxide nanomaterial is recognized as a highly effective photocatalyst due to its favorable chemical stability, physical properties, photoelectric characteristics, abundance. affordability, and non-toxic nature. Nevertheless, the inherent limitations of pure ZnO, such as its substantial band gap, susceptibility to photocorrosion, and rapid internal electronhole pairs recombination generated by absorption of photons, resulting in a significantly reduced efficiency in photocatalysis [48, 49]. Integrating a semiconductor with a narrow band gap emerges as a feasible approach for enhancing the photocatalytic capabilities of ZnO since CdS functions as a visible light catalyst, featuring a band gap of 2.4 eV [5, 50]. However, the use of pure CdS material is prone to significant

photocorrosion, primarily attributed to the oxidation of S² by photogenerated holes. Interestingly, the creation of a CdS/ZnO junction mitigates this issue, showing strong photocatalytic activity for the production of H₂. This heterojunction expands the spectrum response range and enhances the diffusion of charge carriers. The CdS/ZnO heterojunction has attracted considerable attention in research due to its potential uses across various domains, including the production of H₂, sensors, photoresistors, optoelectronic devices, and solar cells. Recently, several methods have been utilized for the fabrication of CdS/ZnO heterojunction, such as coprecipitation, sol-gel, spray pyrolysis, chemical bath deposition, and hydrothermal route [36, 51 - 52]. The microwave synthesis method was employed to create a CdS/ZnO heterostructure, and its structural and morphological properties, as well as photocatalytic properties for H₂ generation, were examined. The findings revealed that CdS particles were adorned onto the single crystal ZnO nanorod surface, with a crystallite size of approximately 43 nm. Notably, the CdS nanoparticle played a significant role in enhancing the heterostructure's photocatalytic H₂ production capability. This enhancement was attributed to increased specific surface area, facilitated separation and migration of photogenerated carriers, and heightened light absorption. In contrast, the band gap of CdS/ZnO is 2.62 eV, which is smaller than that of ZnO, which has a bandgap of 3.09 eV. The CdS/ZnO composite, with a 38 wt% CdS content, exhibits superior hydrogen production, outperforming pure ZnO nanorods and CdS nanoparticles. Furthermore, the composite sample exhibits a specific surface area of 43.375 m²/g, and the prompt photoresponse reaches 130 μ A/cm² [5].

2.1.3. CeO2/CdS

Cerium dioxide (CeO_2) stands out among rare earth oxides and is of significant importance. In recent years, there has been considerable interest in CeO_2 -based photocatalysts, owing to their unique attributes, such as adjustable electronic structures and good photocatalytic activities. Nevertheless, the broad band energy of CeO_2 poses a constraint on its effective utilization of light [18, 53]. A composite of CdS nanowires (NWs) and CeO_2 nanoparticles (NPs) was employed to reduce nitroaromatic compounds to their respective amines (Fig. 1). The reduction reaction took place in a nitrogen (N_2) atmosphere to eliminate oxygen (O_2) supply.

Additionally, ammonium formate was introduced as a hole

scavenger in the reaction. The outcomes surpassed the performance of both blank CdS nanowires and CeO₂ NPs. This work underscores the promising potential of these composites for enhanced photocatalysis applications. The results of the characterization demonstrate that the efficient interaction at the interface and aligned electronic energy levels between one-dimensional CdS nanowires (NWs) and CeO₂ nanoparticles (NPs) enhance the separation and transfer of photoinduced electron-hole pairs. This advancement significantly boosts the photocatalytic efficiency observed in the CdS NWs-CeO₂ NP composites. Additionally, assessments of recycling activity suggest that these composites can function as stable photocatalysts under controlled reaction conditions [54, 55].

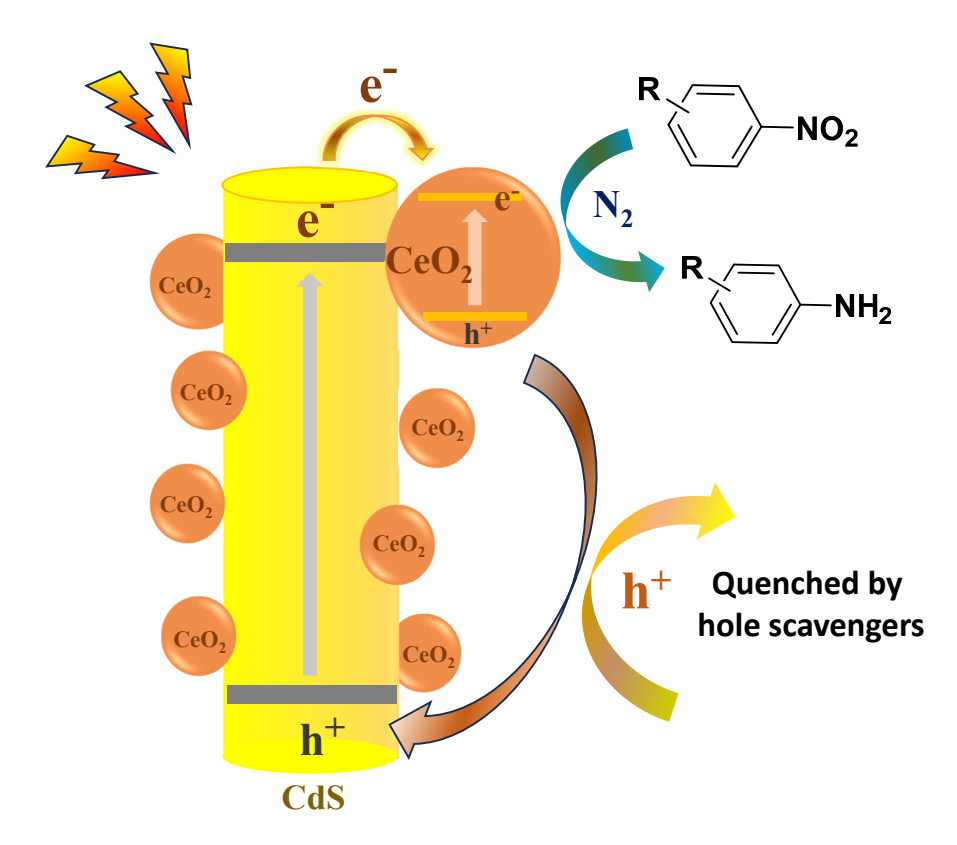


Fig. (1). The composites of CdS nanowires and CeO₂ NPs demonstrate the photocatalytic reduction of nitroaromatics when exposed to visible light irradiation ($\lambda > 420$ nm).

Scheme (3). Photocatalytic selective oxidation of benzyl alcohols over CdS@CeO₂-180.

CdS@CeO₂-180 (where the sample CdS@CeO₂ treated at 180 $^{\circ}$ C) was synthesized using another method and proved to be a versatile photocatalyst, demonstrating high conversion rates and selectivity for the selective oxidation of benzyl alcohols with various substituent groups (o-NO₂, p-OCH₃, p-CH₃ and o-Cl) to corresponding benzaldehydes under visible light for 4h (Scheme 3).

Based on the results, a preliminary mechanism for the photocatalytic benzyl alcohol oxidation over CdS@CeO₂ is suggested (Fig. 2). Under visible light, electrons move from CdS to CeO₂, creating a separation of electrons and holes. Electrons on the CeO₂ surface react with O₂ to form superoxide

anions $({}^{\bullet}O_{2}^{-})$, which contribute to the selective oxidation of benzyl alcohol, while holes are involved in alkoxide oxidation. This process results in the formation of benzaldehyde and hydroperoxide species.

CeO₂ contains Ce with variable valences (Ce⁴⁺ and Ce³⁺), and the Ce⁴⁺/Ce³⁺ couple enhances CdS@CeO₂ photocatalytic activity by efficiently accepting electrons from CdS. This couple also serves as a shallow electron trap, facilitating electron transfer within the CeO₂ shell and promoting the formation of chemisorbed oxygen on the CeO₂ surface, contributing to favorable conditions for the oxidation reaction [6].

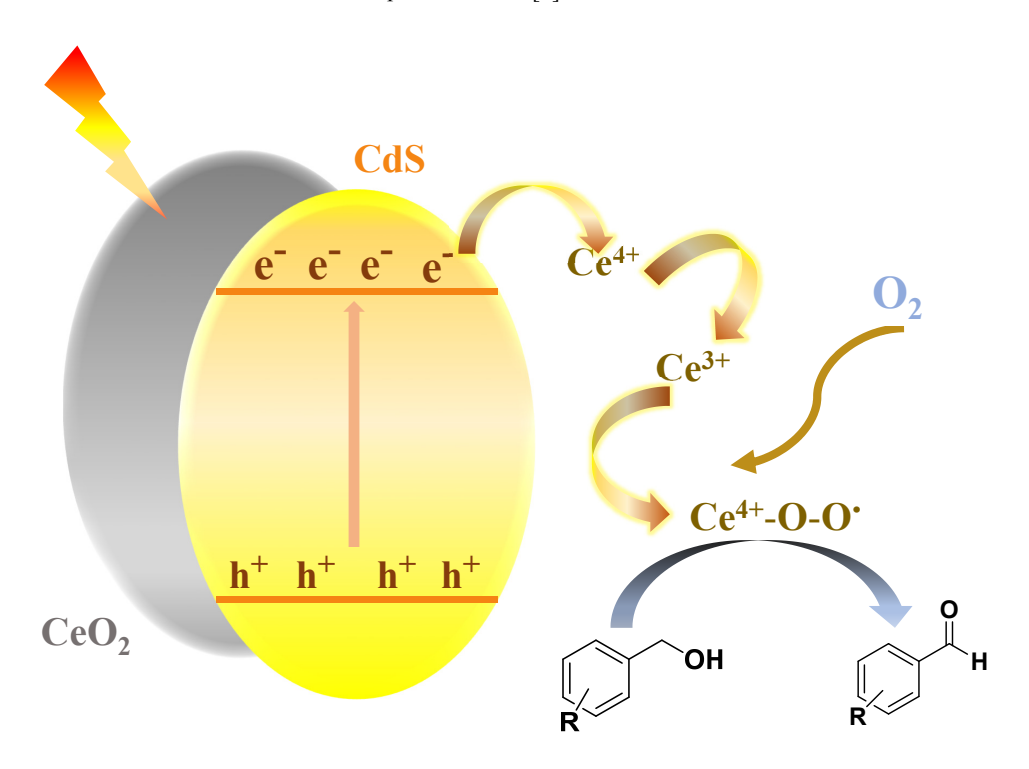


Fig. (2). Suggested reaction pathway for the conversion of benzyl alcohols into their respective aldehydes using CdS@CeO₂-180 under visible-light exposure.

$$R \xrightarrow{\text{II}} N \xrightarrow{\text{NH}_4 \text{SCN, TiO}_2/\text{MoS}_2} R \xrightarrow{\text{II}} N \xrightarrow{\text{N}_4 \text{SCN, 16h, rt, visible light}} R \xrightarrow{\text{N}_4 \text{N}_4 \text{N}_4$$

R=Cl, Br, COOH, OMe, NO₂ etc.

Scheme (4). Photocatalytic thiocyanation of indoles using TiO₂/MoS₂.

2.1.4. TiO₂/MoS₂

Molybdenum disulfide (MoS_2) exhibits promising photocatalytic properties, harnessing sunlight to drive chemical reactions. Its unique two-dimensional structure and bandgap characteristics make MoS_2 a potential candidate for efficient and sustainable photocatalysis, holding significance in various applications, including water splitting, H_2 production, and pollutant degradation. Expansive research has been conducted in recent decades on layered molybdenum disulfide (MoS_2) in the field of photocatalysis due to its minimal band gap (1.3-1.8 eV). This characteristic not only facilitates the absorption of visible light but also ensures remarkable resistance against photocorrosion [7, 56, 57].

A nanocomposite photocatalyst, composed of TiO₂ and MoS₂, was synthesized using a straightforward one-step hydrothermal method. This cost-effective and non-toxic photocatalyst demonstrated excellent efficacy in promoting the thiocyanation of indoles when exposed to visible light at room temperature (Scheme 4). In this, MoS₂ functions effectively as a photosensitizer, and the combined structure demonstrates a synergistic impact, boosting photocatalytic activity when exposed to visible light. The protocol offers advantages such as high isolated yield, compatibility with various substrates, a straightforward workup process, and the catalyst's recyclability. These features make this approach a more practical and

environmentally friendly alternative to established methods.

Based on the aforementioned experimental findings, a potential mechanism for this reaction was suggested (Fig. 3). When subjected to visible-light, the conduction band (CB) of MoS₂ exhibits a more positive nature compared to that of anatase TiO₂, attributable to the quantum confinement effects of MoS₂. Consequently, the photoinduced electrons are transferred to the CB of TiO₂, facilitating the efficient separation of photogenerated electrons and holes. The resulting holes then oxidize thiocyanate anion to form thiocyanate radical, which in turn attacks indole, generating radical intermediate A. Following the oxidation of intermediate A, intermediate B is formed, paving the way for the eventual synthesis of final product 2a through the process of deprotonation [7].

A cost-effective and non-toxic TiO₂/MoS₂ nanocomposite was synthesized using a different procedure and utilized as a highly effective photocatalyst for producing symmetrical disulfides in the presence of visible light at room temperature (Scheme 5). The reaction conditions were compatible with both alkyl and aryl thiols, resulting in an excellent yield of the respective disulfides. The recovery of the photocatalyst was very simple, involving basic centrifugation and filtration, enabling multiple reuses without a significant reduction in its activity.

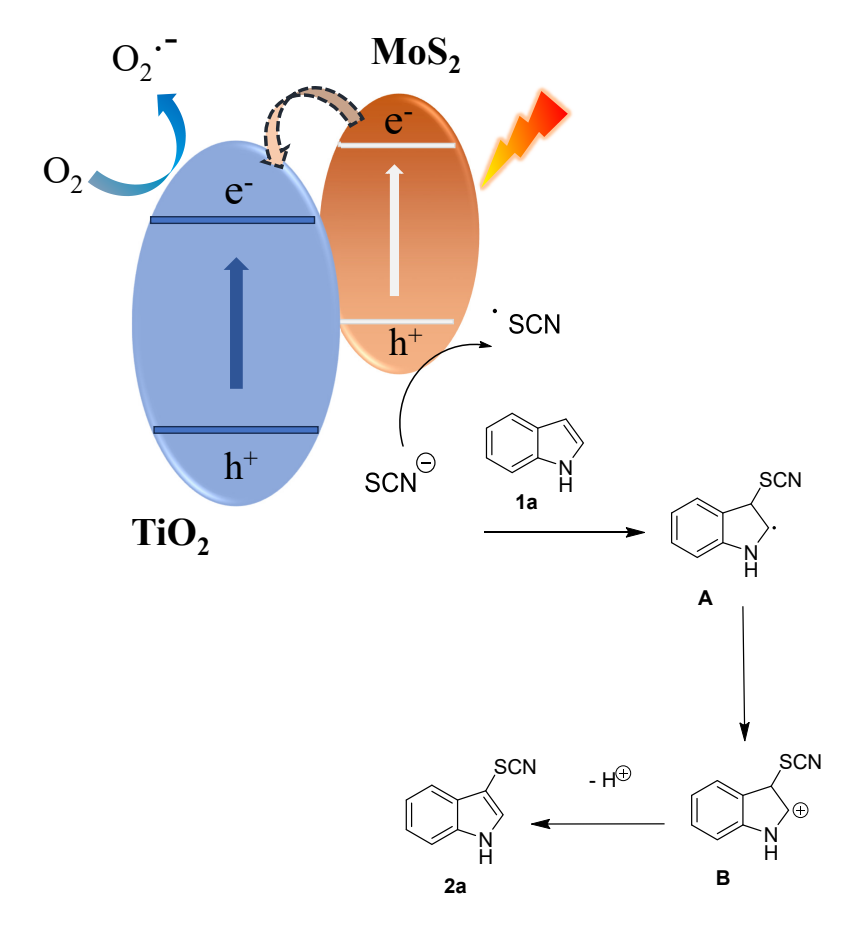


Fig. (3). Proposed photocatalytic pathway for Photocatalytic thiocyanation of indoles using TiO₂/MoS₂.

$$\begin{array}{c} \text{SH} & \frac{\text{TiO}_2/\text{MoS}_2}{\text{EtOH, Visible light, rt}} \\ \end{array}$$

R= H, Cl, F, OMe, Br etc.

Scheme (5). Formation of symmetrical disulfides using TiO₂/MoS₂ in the presence of visible light.

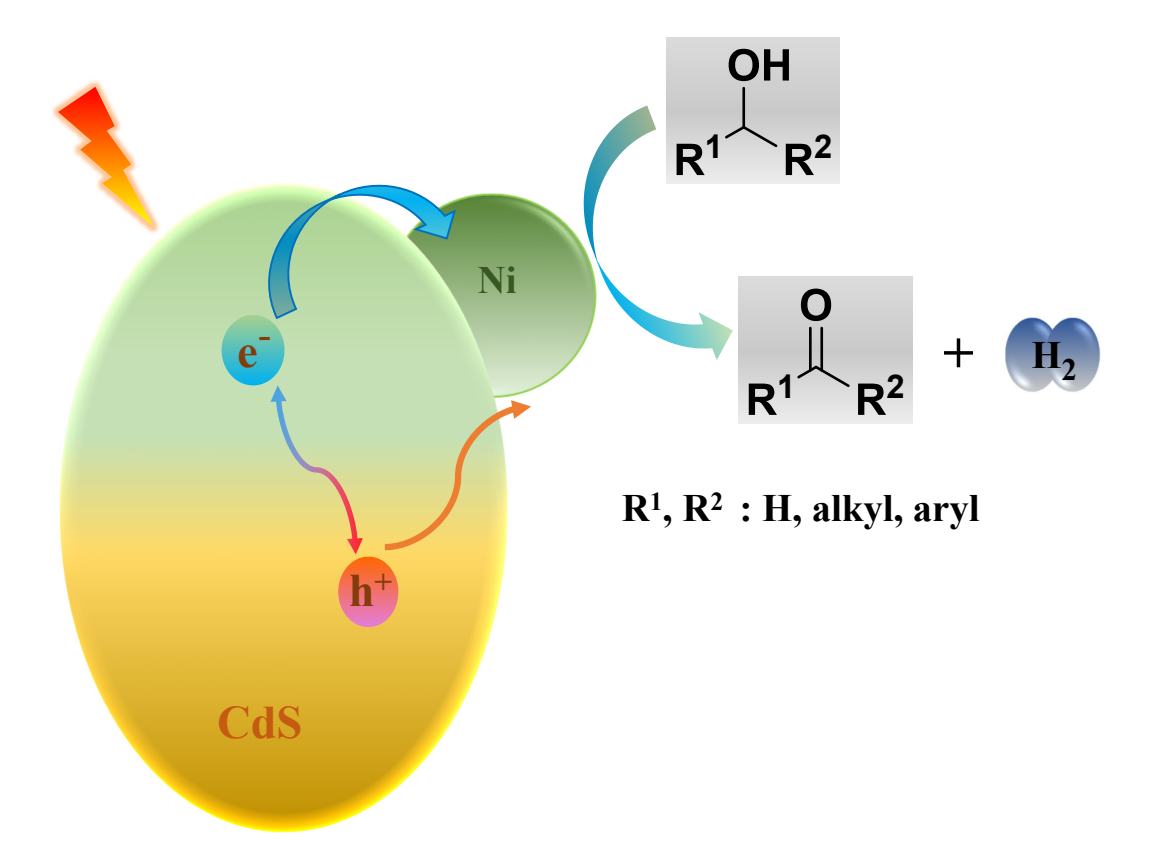


Fig. (4). Alcohol splitting over Ni/CdS in the presence of visible light.

The photocatalytic activity of the TiO₂/MoS₂ nanocomposite was explored using 4-chlorothiophenol as a model substrate. While anatase TiO₂ showed no reactivity, pure MoS₂ produced a 48% yield of the desired product in ethanol. The TiO₂/MoS₂ heterojunction (Molar ratio of Ti to Mo is 10:1, 10 mg) emerged as the most effective catalyst, providing almost quantitative yield for the desired product. However, the choice of solvent significantly influenced the reaction yields, with various solvents, such as CH3CN, DCM, DMF, toluene, and water, leading to decreased product yields. Furthermore, the desired product was not observed in the absence of visible light and catalyst (TiO₂/MoS₂), underscoring the significance of the photocatalytic system. Subsequent investigations indicated that

the presence of air or oxygen significantly influenced the rate of the reaction [58].

2.2. Metal Chalcogenide Heterostructure Nanoparticles

Metal ions are being increasingly employed as cocatalysts because of their facile integration onto photocatalysts and the establishment of close interfacial connections through electrostatic attraction. The integration of metal nanoparticles with chalcogenides has garnered significant attention in the realm of photocatalysis. When chalcogenides are combined with metal nanoparticles, such as Co, Ni, Cu, Zn, Pd, etc, these composites exhibit synergistic effects that enhance their overall performance. This integration over advantages such as

plasmonic effects, efficient charge carrier separation, and the introduction of co-catalytic activity, resulting in tunable and stable materials ideal for a range of photocatalytic processes. Researchers have investigated various heterogeneous catalysts like Ni/CdS, Zn/CdS, Co/CdS, and Pd/CdS for diverse photocatalytic applications. The photocatalytic activity, as well as the photocatalytic mechanism of these photocatalysts, are explained in the following section [59-62].

2.2.1. Ni/CdS

A heterogeneous photocatalyst Ni/CdS (Ni nanocrystal modified CdS nanoparticles) was synthesized. The photocatalyst has shown effective dehydrogenation of alcohols into corresponding aldehydes or ketones under ambient conditions using visible light (Fig. 4). The optimized AQYs (apparent quantum yields) reached 46%, 38%, and 48% under visible light exposure (at 447 nm) for the dehydrogenation of ethanol, methanol, and 2-propanol respectively. With a higher value of TON (Turnover number) (>44,000) in 2-propanol dehydrogenation, this catalyst sets a remarkable value for photocatalytic liquid alcohol splitting. Additionally, this catalyst system exhibits excellent performance with various aliphatic and aromatic alcohols, providing the corresponding carbonyl compounds with high conversion rates and remarkable selectivity. It was reported that the interaction of Ni nanocrystals with CdS nanoparticles plays an important role in

the photocatalytic mechanism process of alcohol splitting.

From the experimental findings, a photocatalytic mechanism for the dehydrogenation of alcohols was proposed (Fig. 5). At first, the absorption of alcohol on the Ni particle surface occurs, resembling a step in the process of thermal catalytic mechanism of dehydrogenation. A photoinduced electron-hole pair is generated upon CdS exposure to highenergy photons, and then the photoexcited electrons move from CdS to Ni, reducing the proton from OH of the alcohol molecule that is absorbed on the surface of Ni. This results in the formation of a Ni-H hydride and an alkoxide anion. Subsequently, the alkoxide undergoes oxidation, leading to Niassisted cleavage of a C-H and the formation of aldehyde or ketone. Ultimately, the generation of a single hydrogen molecule is achieved through the interaction of two Ni-H hydrides. The rate-limiting step is the oxidation half-reaction, as indicated by Kinetic Isotope Effect (KIE) results and dissociation energy differences between O-H and C-H [8, 64].

The same catalyst Ni/CdS was synthesized by using different methods and used for the production of imines under visible light irradiation (Scheme 6). The method involves a photocatalytic non-oxygen coupling reaction of various amines, with a significant enhancement facilitated by $\rm H_2$ evolution using noble-metal free Ni/CdS NPs (nanoparticles) in the presence of H₂O.

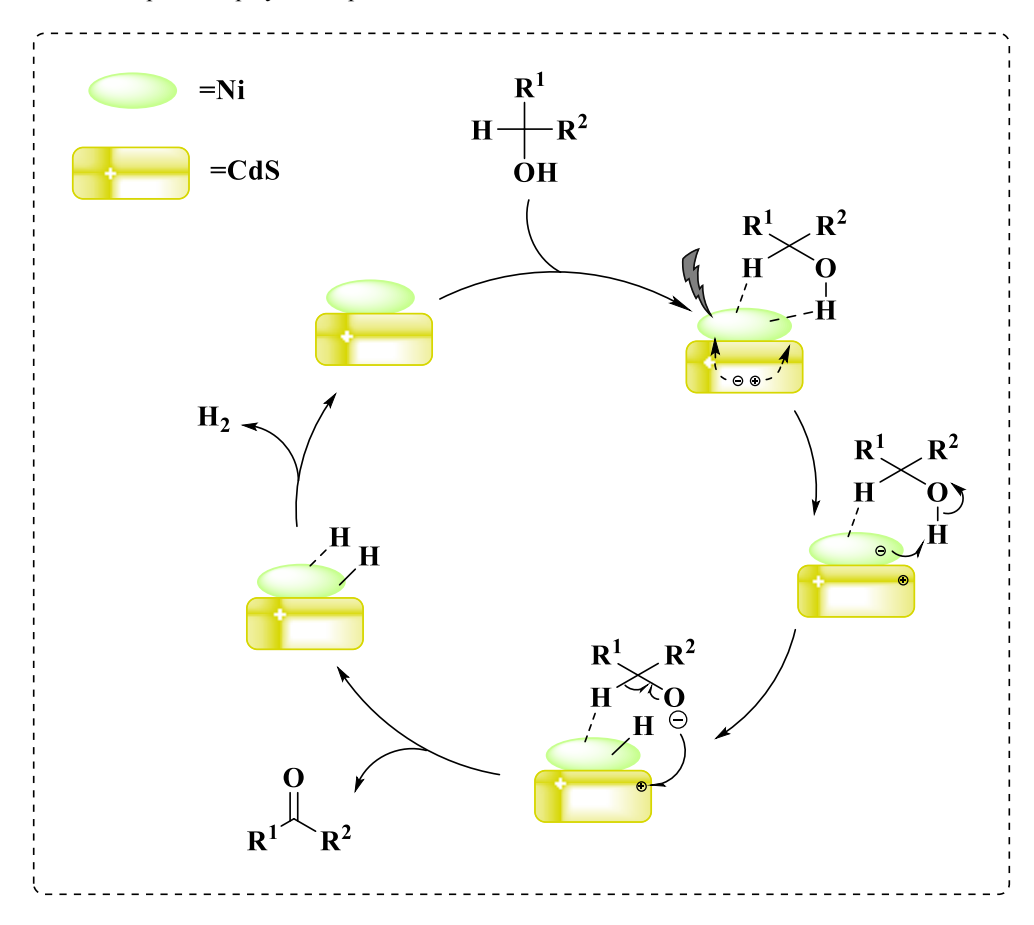


Fig. (5). Proposed photocatalytic mechanism for alcohol splitting by Ni/CdS.

Scheme (6). Photocatalytic non-oxygen coupling reaction of amines using Ni/CdS.

The catalyst demonstrates remarkable performance, achieving a 99% conversion of benzylamine with a 97% selectivity for imine in the non-oxygen transformation process. This reaction is accompanied by the production of hydrogen with a maximum evolution rate of 21.4 mmol g-1 h-1 (λ >420 nm). This underscores the efficiency of the catalyst in concurrent hydrogen evolution. Ni/CdS catalyst proves to be more effective in promoting the photocatalytic coupling of benzylamine to imine than that of the other metal catalysts, such as Co/CdS, Fe/CdS, Au/CdS, and Pt/CdS. When g-C₃N₄ is used as a support instead of CdS, only 5% benzylamine conversion and 85% imine selectivity, along with minimal H₂ production, are achieved. The synergy between Ni NPs and CdS is crucial for enhancing photocatalytic performance facilitating the production of H₂ from water splitting. Ni acts as an active sites for the evolution of hydrogen on the CdS

photocatalyst, promoting the consumption of photoinduced electrons and activating substrates. The different substrates of aryl amines have shown excellent activity and selectivity, resulting in the formation of their corresponding imines. This process has been accompanied by remarkable hydrogen evolution activity, underscoring the effectiveness of the innovative approach developed in this study [8, 64].

A plausible photocatalytic mechanism was suggested for the H₂ production with the nonoxygen coupling of benzylamine to imine in the presence of H₂O (Fig. 6). Under light irradiation, electrons from VB of CdS transfer to its CB, creating holes at the VB. These electrons then reduce aqueous protons to form H₂ on Ni nanoparticles, while the carbon cationic species from holes react with benzylamine, producing the respective imine [8, 64].

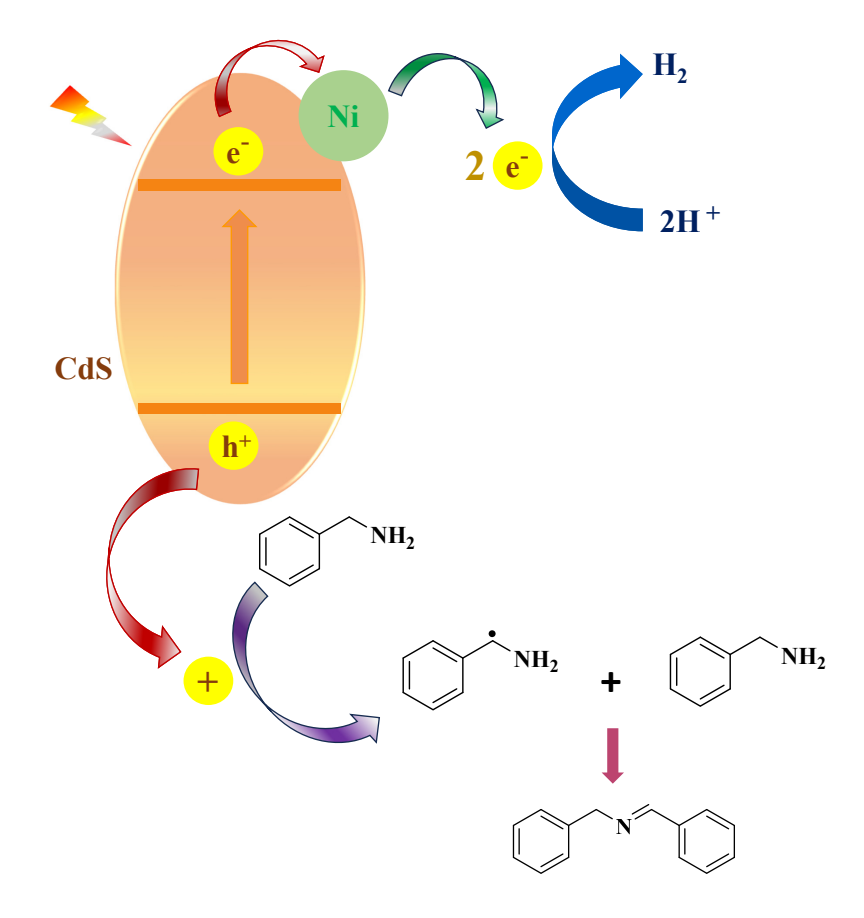


Fig. (6). Proposed photocatalytic mechanism over Ni/CdS NPs.

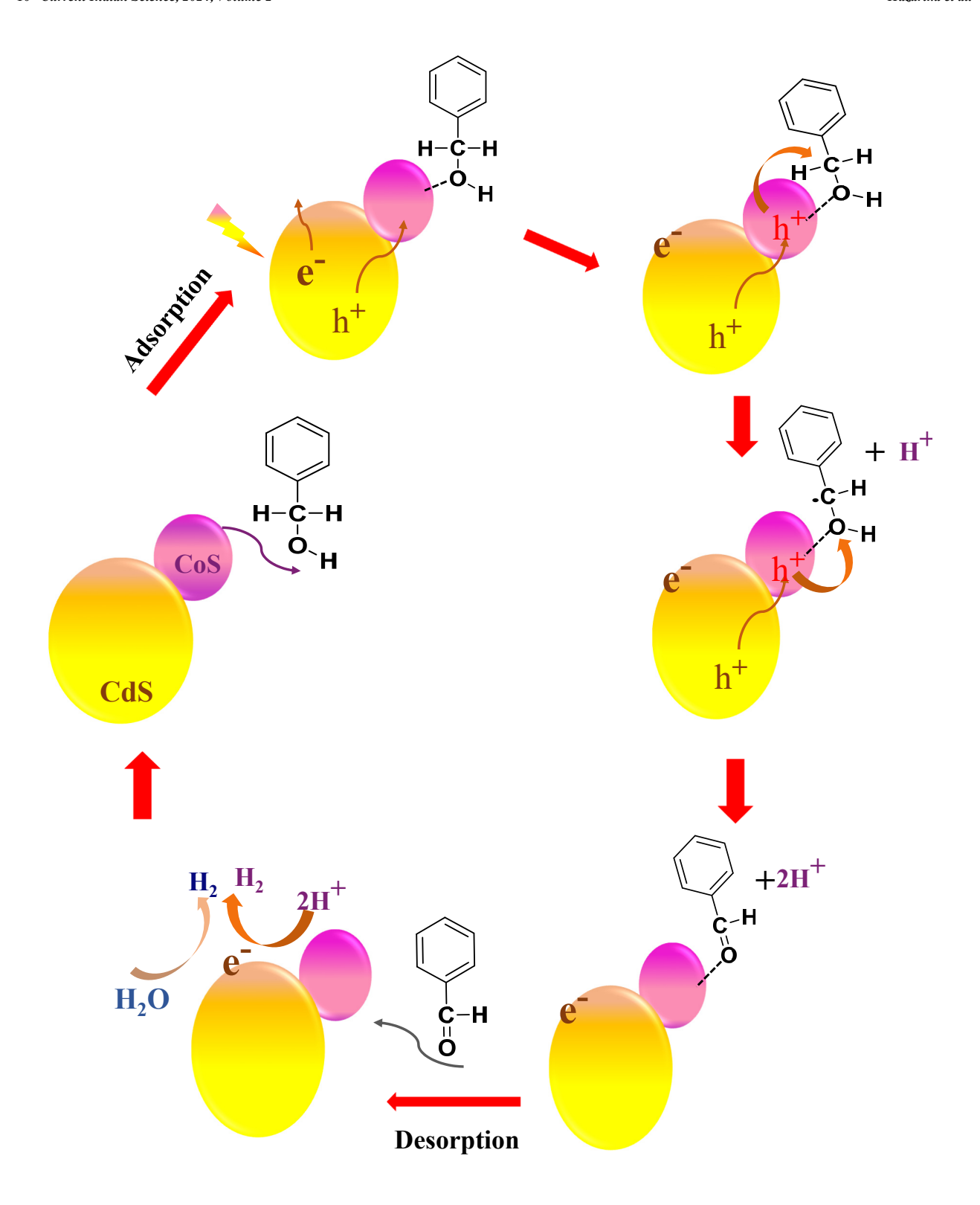


Fig. (7). Proposed mechanism for the photocatalytic generation of hydrogen, combined with the selective oxidation of benzyl alcohol to benzaldehyde over Co-CdS-W.

2.2.2. Co/CdS

Co-modified CdS quantum dots (QDs) were effectively synthesized using a straightforward solvothermal technique, followed by subsequent processes of ligand exchange and the photodeposition of Co²⁺. These modified QDs exhibit

remarkable performance in photocatalytic processes, particularly in hydrogen (H_2) evolution and selective oxidation of benzyl alcohol to benzaldehyde (Fig. 7).

The incorporation of CoS enhances visible light absorption, contributing to increased H₂-production activity

and benzaldehyde productivity. Notably, the photocatalytic system achieves high benzaldehyde selectivity, preventing further oxidation to benzylacetate. The Density functional theory (DFT) analysis also indicates the higher photocatalytic activity of the Co-modified CdS-W (CdS-W are water soluble CdS QDs) than that of the CdS-W. This work provides insights into developing photocatalytic systems that efficiently produce H₂ and synthesize valuable organic compounds [9].

2.2.3. Zn/CdS

Zinc-doped cadmium sulfide (CdS) was synthesized using an eco-friendly and simple solvothermal method. Following the doping process, a noticeable red shift was observed, particularly with higher amounts of zinc. This suggests that the inclusion of zinc has a substantial impact on the optical characteristics related to light absorption in the synthesized catalyst. The resulting photocatalyst exhibits enhanced stability in facilitating the efficient photodegradation of methylene blue (MB) dye [65].

2.2.4. Cu/CdS

The hierarchically structured novel Cu/CdS nanorods were synthesized using an ecofriendly photo deposition method which demonstrated promising potential as a photocatalyst for the degradation of various classes of dye [10].

2.2.5. Pd/CdS

A coenocytic Pd@CdS nanocomposite was successfully synthesized using a simple wet chemistry method. The study revealed well-distributed Pd nanoparticles within the CdS shell, forming a coenocytic nanostructure. The growth process depends on precursor concentration, which is the inherent characteristic of noble metal colloids. The photocatalytic performance of Pd@CdS under visible light was assessed by selectively oxidizing various alcohols using O₂ as an oxidant under mild conditions. The nanocomposite exhibited high photocatalytic activity compared to blank-CdS, attributed to increased light absorption, prolonged lifetime of photoinduced charge carrier, and favorable adsorption. It was reported that coenocytic Pd@CdS nanocomposite exhibited approximately 31% conversion and 30% yield for benzyl alcohol to benzaldehyde, respectively, when exposed to visible light for 4 hrs, surpassing the outcomes observed with blank-CdS (16% conversion and 15% yield). This pattern holds true for the selective oxidation of various alcohol substrates. In conclusion, the coenocytic Pd@CdS nanocomposite shows promise for efficient visible light photocatalysis [11, 66, 67].

A photocatalytic mechanism was proposed for the selective oxidation of alcohols using the synthesized catalyst, as shown in Fig. (8). When CdS exposed to visible light, the electrons in the CdS shell are elevated to the CB, creating holes in the VB. These photoinduced electrons are captured by the Pd metal cores within the CdS, extending the lifetime of photogenerated charge carriers. Concurrently, the holes react with the adsorbed alcohols, generating radical cations. These cations then undergo further reactions with O2 or O2 radical species, resulting in the formation of corresponding aldehydes [11, 66,

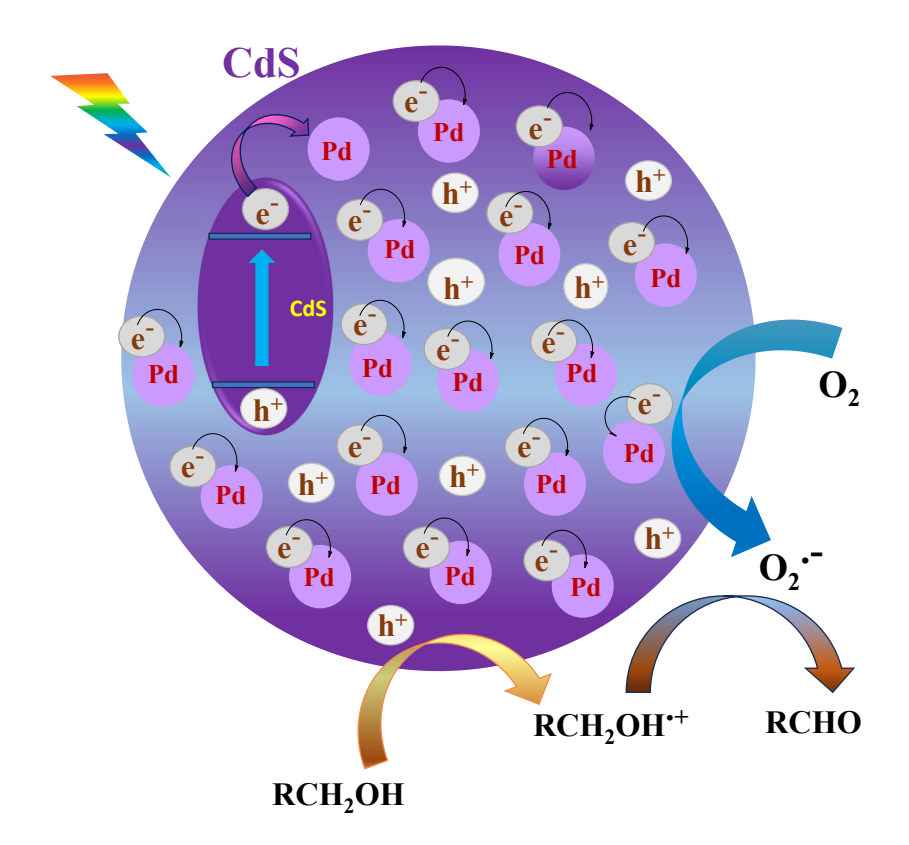


Fig. (8). Proposed photocatalytic mechanism for selective oxidation of alcohol on Pd@CdS nanocomposite.

This study is anticipated to offer valuable insights for creating additional core-shell nanocomposites, thereby paving the way for their application in the realm of photocatalytic selective organic transformations [11, 69].

3. NEW AGE METAL CHALCOGENIDE HETEROSTRUCTURES

The photocatalytic efficiency of a catalyst can be enhanced effectively by precise modulation of interfacial contact of heterojunction photocatalysts and regulation of photoexcited charge carriers. Based on this concept, a 2D/2D CdS/g-C₃N₄ nanocomposite photocatalyst resembling a p-n junction with a Z-scheme mechanism was developed. It has been observed that pure g-C₃N₄ exhibits poor conversion but moderate selectivity for photocatalytic DFF (2,5-diformylfuran) production, and CdS alone exhibits high conversion but poor selectivity for the same. However, however, the composite of CdS and g-C₃N₄ provides the combined benefits of both types of catalysts [12 -16]. A combination of an appropriate amount of components and good dispersion are responsible for creating an enhanced heterojunction effect, resulting into better photocatalytic activity. From the DFT calculations, it was revealed electron transfer and separation followed a Z-scheme mechanism, which maintains a high redox capacity and consequently results in high photocatalytic activity. In the CdS/g-C₃N₄ nanocomposite, g-C₃N₄ behaves as an n-type semiconductor and CdS as a p-type semiconductor, thus resulting in p-n heterojunction. An electric field develops in the opposite direction to that of holes in VB and parallel to the direction of electron flow in the CB, thus giving rise to a Z-scheme [69]. CdS/g- C₃N₄ composite is also found to selectively oxidize alcohols to aldehydes and reduce nitrobenzene to aniline when irradiated with visible light under the N₂ atmosphere. It was concluded from their work that holes were responsible for the benzyl alcohol oxidation to benzaldehyde, whereas the electrons caused the reduction reaction of nitrobenzene to aniline. 1-10wt% loading of CdS was found to be suitable for catalyzing the reaction efficiently as an excess of it decreases its contact with visible light and minimizes the intensity of the light in the deep reaction solution and hence decreases the photocatalytic activity [70 - 73].

 $Cd_3(C_3N_3S_3)_2/CdS$ composite is a highly porous heterostructure that was developed via hydrothermal method. This method weakens and breaks down the Cd-S bonds to release Cd^{2+} ions into water. Nitrogen oxide and CO gases are released when the triazine ring structure of $Cd_3(TMT)_2$ breaks down in a hydrothermal process, ultimately giving rise to a large number of pores. The composite proved to show high photocatalytic activity toward selective oxidation of toluene to

benzaldehyde (Scheme 7).

The absence of a solvent makes this reaction more environment friendly. The catalyst is found to be highly stable, and the microporosity in the composite leads to an increase in the absorption of light, which leads to enhanced photocatalytic activity. When visible light strikes the surface of the composite, electron-hole pairs are generated. The electron flows from the conduction band (CB) of the Cd₃(TMT)₂ to the CB of the CdS, and the holes travel from the valence band (VB) of the CdS in the reverse direction. The holes oxidize the toluene to cationic radical, and the adsorbed oxygen molecule takes up the electron and forms O_2^- radical. The superoxide radical then oxidizes the cationic radical and forms the targeted product benzaldehyde [74].

The different morphologies of CdS, when combined with TNT (Titanate nanotubes), give rise to enhanced photocatalytic activity [75 - 77]. Nanotube, being one dimensional, provides a large surface-to-volume ratio, which helps in separating the photogenerated electron hole-pair. They have a large surface area, which increases their capacity to absorb light as compared to the bare CdS. TNT has a wide band gap, which restricts its utilization in the visible range. It has a large surface area, but due to its wide band gap, its application is limited. Therefore, it was coupled with CdS to form a CdS/TNT nanocomposite with a narrow band gap. The CdS/TNT nanocomposite was synthesized by using a one-step, in-situ hydrothermal method (Fig. 9). The photocatalyst so developed was used in the selective aerobic oxidation of allylic and benzylic alcohol. BET confirmed the presence of pores, which seem to increase the absorption of substrate compared to blank CdS. No hydroxyl radical is formed, as confirmed by adding a hydroxyl scavenger, which does not affect the reaction at all. When the composite is irradiated with visible light, an electron from the valence band of CdS goes to the CB of CdS, which is then taken up by the CB of TNT, consequently preventing the recombination of electron-hole pair (Fig. 9) [75].

MOF and MOF derivatives are highly versatile photocatalysts as both the metal nodes and organic linkers individually can behave as semiconductors. They serve as an excellent template for developing composites with metal chalcogenides owing to their high specific surface area, porous nature, restricted electron-hole recombination, etc [31]. CdS -MIL 68 was used in the reduction of 4-nitroaniline to phenylenediamine (PPD) with water as a solvent and under visible light of wavelength >420nm. Metal-organic frame work (MOF) supported CdS enhances the photocatalytic activity as compared to a hybrid because of its ultra-high surface area. MOF not only behaves as a host for supporting metal chalcogenides but also helps maintain the charge separation of photogenerated charge carriers. Photogenerated electrons and holes act as active species for the reaction, and HCO2NH4 was added as the hole scavenger (Fig. 10) [20].

CH₃
$$\frac{\text{Cd}_3(\text{C}_3\text{N}_3\text{S}_3)_2/\text{CdS}}{300 \text{ W Xe lamp > 420nm}} + \frac{\text{O}}{\text{H}}$$

Scheme (7). Photocatalytic conversion of Toluene to benzaldehyde using Cd₃(C₃N₃S₃)₂/CdS.

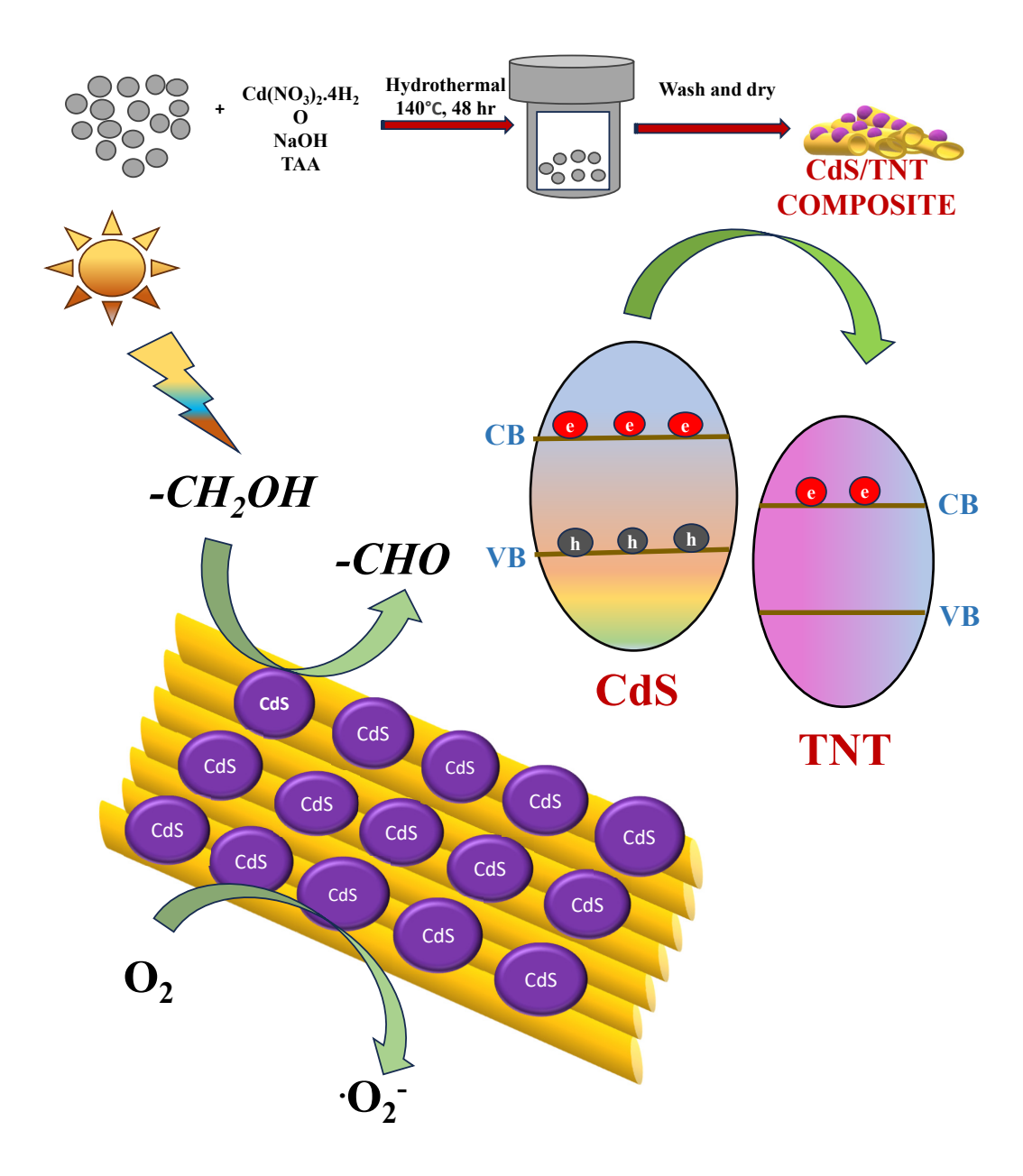


Fig. (9). A schematic illustration for preparation of CdS/TNT nanocomposite via in-situ hydrothermal process along with a proposed mechanism for photocatalytic selective oxidation of alcohol to corresponding aldehydes over the surface of CdS/TNT nanocomposite.

Single-atom catalysts have gained a lot of attention in recent years owing to the innumerable advantages ranging from 100% atom utilization in unsaturated coordination sites to enhanced photocatalytic activity [19, 78]. However, most of the reported single-atom catalysts have very low loading of active metal centers onto the surface of the supports. The most common strategy to develop highly efficient single-atom photocatalysts involves the reduction of metal content and precise control over surface defects and voids. However, new hassle-free strategies and materials need to be explored to increase the metal loading over the support. It has been observed that manipulation of the basal plane of transition metal chalcogenides introduces new defects that can accommodate a considerable number of catalytically active single metal atoms. Keeping in view the advantages associated with the use of 2D layered transition metal chalcogenides for energy applications and petrochemical conversion, the transition metal chalcogenide was exfoliated by treating it with n-BuLi solution. Such exfoliation results in anionic vacancy sites, which can accommodate a high density of single atoms. Using this strategy, MoS₂ with 10 wt% Fe single atom loading was developed successfully by following the scheme illustrated in Fig. (11), which exhibited excellent catalytic properties for reverse water gas shift reaction with selectivity as high as 99.9% [19]. Such metal chalcogenide-based single-atom catalysts are often used for the conversions of small molecules, but there is an urgent need to explore its application in other industrially important organic transformations.

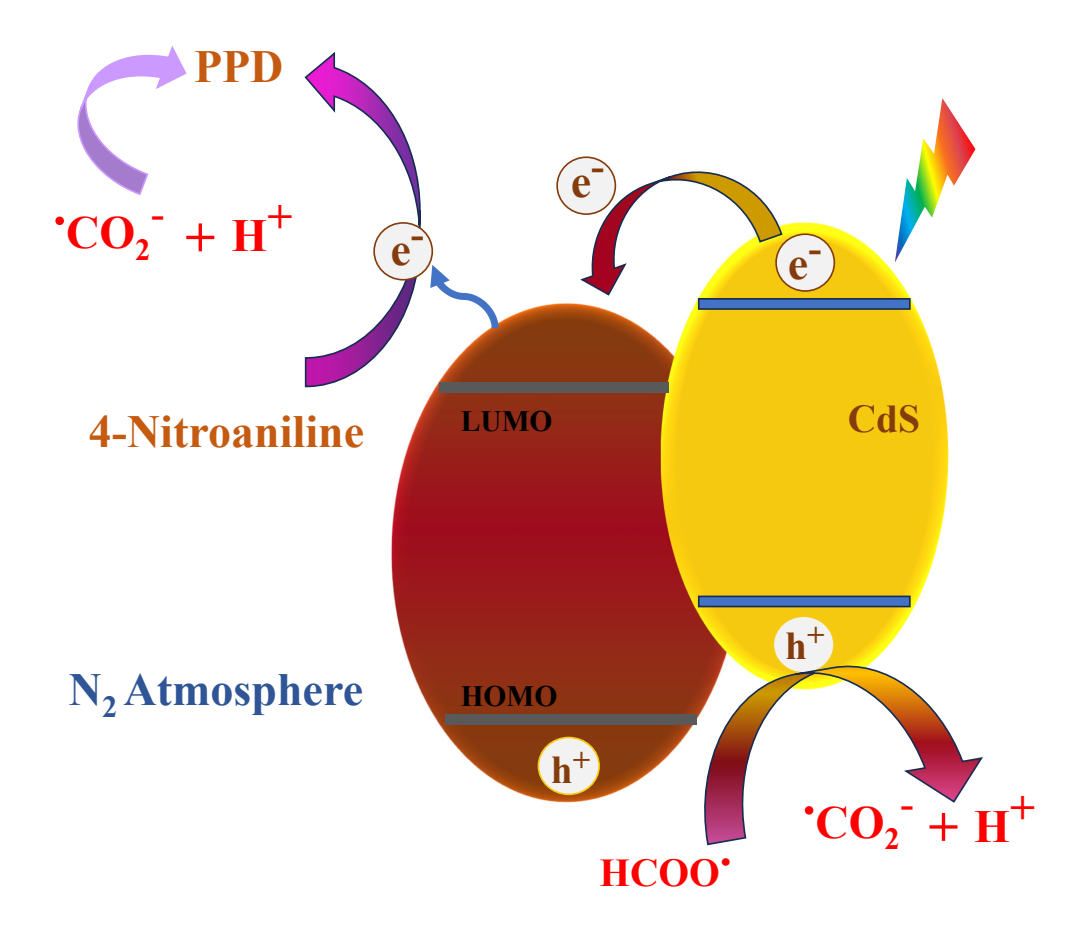


Fig. (10). Photocatalytic mechanism for 4 nitroaniline reduction to PPD (phenylenediamine).

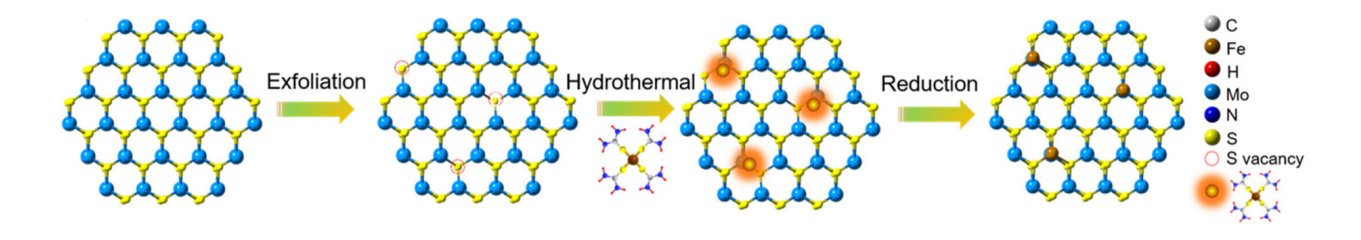


Fig. (11). A Schematic illustration of the preparation of metal chalcogenide-based SAC. Reprinted with permission from ref [19]. Copyright (2019), ACS Catal.

4. BOOSTING STABILITY AND PHOTOCATALYTIC EFFICIENCY OF METAL CHALCOGENIDES WITH MEDIATORS

Various heterostructures of metal chalcogenides have been synthesized using different materials to enhance the photocatalytic activity of the metal chalcogenide semiconductor. However, certain limitations persist in these heterostructures, which results in a reduction in the transfer of photogenerated charge carriers and, consequently, diminishing the overall photocatalytic activity. To address these challenges, electron mediators have been incorporated into a Z-scheme configuration to enhance photocatalysis. The subsequent discussion addresses alterations in photocatalytic performance when employing mediators like nitrate, EDTA, non-conjugated polymer, etc., in conjunction with metal chalcogenides.

4.1. Nitrate as a Mediator

Since CdS nanowires are excellent catalysts for the oxidation of benzyl alcohol due to their one-dimensional structure and large surface area. The catalytic properties of CdS nanowires can be further enhanced by the addition of nitrate salt, which acts as a redox mediator in the solution. The mediator facilitates faster charge transfer processes, prevents recombination, and enhances photocatalytic activity, leading to high-yield conversion and selectivity. In this study, researchers utilized nitrate salts of lithium, calcium, magnesium, and manganese as mediators in the photocatalytic selective oxidation of benzyl alcohol to benzaldehyde and the oxidation of 5-hydroxymethylfurfural. The selectivity and conversion of benzyl alcohol are both above 99%, with a yield rate of up to 13.6 mM•h⁻¹.

Fig. (12). Proposed mechanism for LiNO₃ mediated photocatalytic oxidation of benzyl alcohol.

Based on a sequence of experimental results, a mechanism was proposed for the formation of benzaldehyde, which involved the generation of a nitrate radical (Fig. 12). The alcohol substrates were oxidized by this nitrate radical instead of the photogenerated holes. Along with the oxidation of benzyl alcohol, this nitrate radical facilitates HMF oxidation for selective production of 2,5-diformylfuran. It was worth mentioning that tetrabutylammonium cations did not work well with nitrate-based catalysis because of the weaker interaction of nitrate. These findings have demonstrated the utility of basic nitrate salts in facilitating oxidations relevant to biomass enhancement. Moreover, they have introduced both new opportunities and challenges for further exploration of mediated photocatalysis [79].

4.2. Using EDTA in CdS/g- C_3N_4 Heterostructure as Mediator

The CdS-EDTA/g- C_3N_4 heterostructure was designed by growing CdS on g- C_3N_4 nanoflakes in a hydrothermal process, with the aid of the EDTA, which acts as a chelating agent (Fig. 13).

A Z-scheme photocatalytic mechanism was suggested for the CdS-EDTA/CN heterostructure based on the experimental findings, where the chelating agent EDTA mediates electrons between the CdS nanoparticle and g-C₃N₄ nanoflakes. EDTA behaves as a binder between these semiconductors and also affects the morphology of the CdS [18, 19, 80].

In the photocatalytic reduction of p-NP, it converts to p-nitrophenolate ions (reaction 1), and N_2H_4 oxidizes to N_2 and H^+ (reaction 2). The oxidation of N_2H_4 is initiated by h^+ from the VB of CdS. Simultaneously, p-nitrophenolate ions undergo hydrogenation reduction to produce p-aminophenol (reaction 3), which occurs through the acquisition of H^+ and e- from the CB of g- C_3N_4 . For the selective oxidation of benzyl alcohol, it is converted to carbocationic radicals (reaction 4), reacting with O_2 radicals to form benzaldehyde and H_2O_2 (reaction 6). Here, the O_2 radical is formed by the reaction of adsorbed O_2 molecule with the e- generated from the CB of g- C_3N_4 (reaction 5). The photocatalytic system minimizes OH radical generation, ensuring high selectivity in benzaldehyde production and preventing overoxidation of benzyl alcohol (Scheme 8).

Scheme (8). Reactions (1), (2), and (3) are p-nitrophenol reduction, and reactions (4), (5), and (6) are selective oxidation of benzyl alcohol.

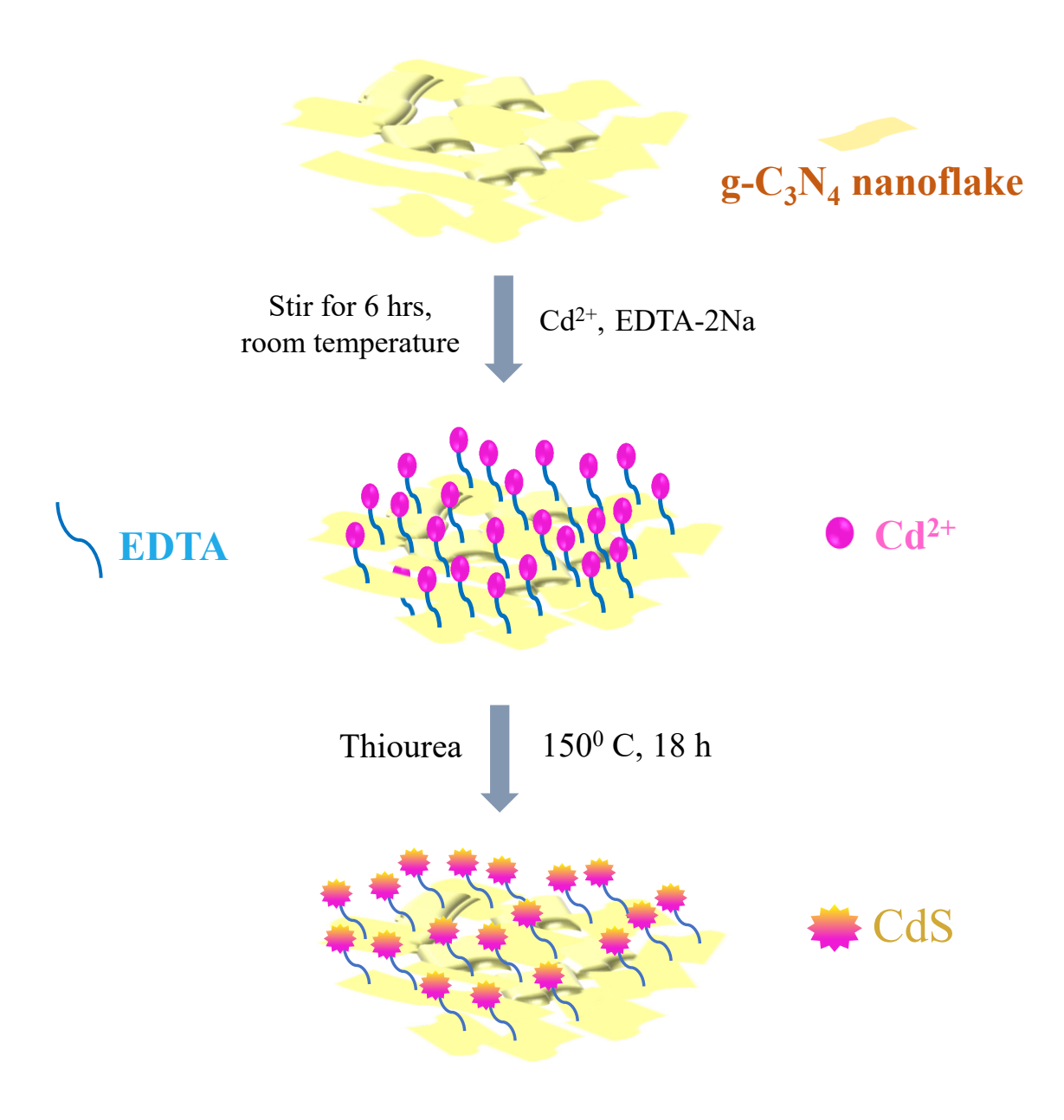


Fig. (13). Diagram depicting the formation process of CdS-EDTA/CN heterostructures.

The CdS-EDTA/CN photocatalysts gain a notable advantage in capturing visible light, accelerating the separation of electron-hole pairs, and maintaining high photoredox potentials due to the integration of three components. Consequently, the performance of CdS-EDTA/CN photocatalysts is improved in the context of nitrophenol reduction and benzyl alcohol oxidation in photoredox reactions [80].

4.3. Unleashing Non-conjugated Polymers as Charge Relay Mediators

A highly effective and versatile electrostatic self-assembly approach was introduced for the intricate construction of TMCs/PDDA/MQD (TMCs: ZnIn₂S₄, CdS, CdIn₂S₄, and In₂S₃,

PDDA (poly (diallyldimethyl ammonium chloride)) is a polymer, MQDs are MXene quantum dots) photosystems with continuous pathways for charge transfer. This approach facilitates visible-light-driven selective nitroaromatics reduction to amino aromatics and photocatalytic H_2 production (Scheme 9).

The inclusion of PDDA, which is a solid-state ultrathin non-conjugated polymer, plays an important role by showing electron-withdrawing capability and facilitating the unidirectional flow of electrons from TMCs to MQDs. The MQDs capture the electrons and increase the transfer of electrons. This results in a directional charge transfer cascade, extending the lifetime of charges in TMCs [17, 18. 81].

$$R \xrightarrow{NO_2} \frac{\lambda > 420 \text{ nm}}{N_2, 298 \text{K, water}} R \xrightarrow{NH_2} NH_2$$

Scheme (9). Selective nitroaromatics reduction to amino aromatics under visible light.

5. FACTORS INFLUENCING THE PHOTOCATALYTIC ACTIVITY OF METAL CHALCOGENIDES AND THEIR HETEROSTRUCTURES

Heterogeneous catalysis seems to be enormously potent for enhancing photocatalytic activity, but it still suffers from a smaller number of catalytically active sites and poor interface. The glass transition temperature (T_g) of chalcogenides is an extremely crucial property for determining the stability and structural integrity of the photocatalysts. It is the continuous

alloying and the network of covalent bonds that establish this structure and property relationship. Ge_xSe_{1-x} is a chalcogenide glass that exhibits excellent optoelectronic properties, and the determination of its glass transition temperature (T_g) is very important for knowing about its optoelectronic properties. Multivariate linear regression (MLR) has been developed for that purpose, and it seems to reproduce highly accurate glass transition temperature (T_g) at a much faster rate [82].The variation in the morphology (Fig. 14). In the phase of metal chal-

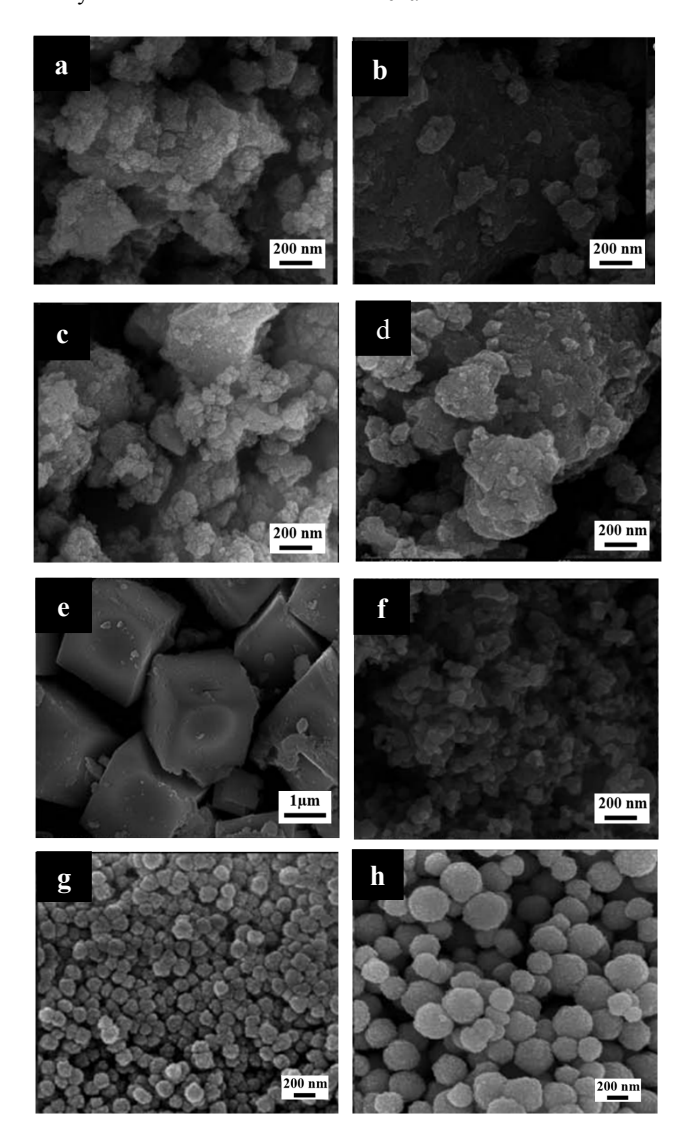


Fig. (14). SEM images of the CdS samples: CdS-S1 (a), CdS-S2 (b), CdS-S3 (c), CdS-S4 (d) and CdS-S5 (e); typical SEM images of commercial CdS (f), spherical CdS-1 (g) and spherical CdS-2 (h) are also shown. Reprinted with permission from ref [83]. Copyright (2012), *Chem. Sci.*

cogenide, the semiconductor also leads to variation in the band gap of the semiconductor, which may lead to different delocalization and mobilization of the photogenerated charge carrier, eventually leading to raised photocatalytic activity. Many products like benzyl alcohol, benzaldehyde, and benzoyl benzoate are required by industries ranging from pharmaceutical, dye stuff, perfumes, *etc.*, which are produced by oxidizing toluene. When the visible light strikes the surface of the cubic phase sheet, electrons and holes are generated, which get separated. The toluene gets adsorbed on the surface of the semiconductor and gets oxidized to cation radical due to

oxidation by holes, and molecular oxygen takes up the electron to form the superoxide radical, which then selectively oxidizes the toluene radical to form the required product benzaldehyde [33, 83, 84].

Reaping the benefits of morphological impact, a surfactant-assisted hydrothermal technique was used to develop a CdS flower for photocatalytic selective reduction of nitro aromatic compound and C-H oxidation (Scheme 10). Decanoic acid and potassium ortho ethyl xanthate were used as the ligand and precursor of Sulphur, respectively, and water was used as the solvent to prepare the ultrathin CdS flower of 0.8 nm thickness.

Scheme (10). Photocatalytic selective reduction of nitro aromatic compound using CdS flower.

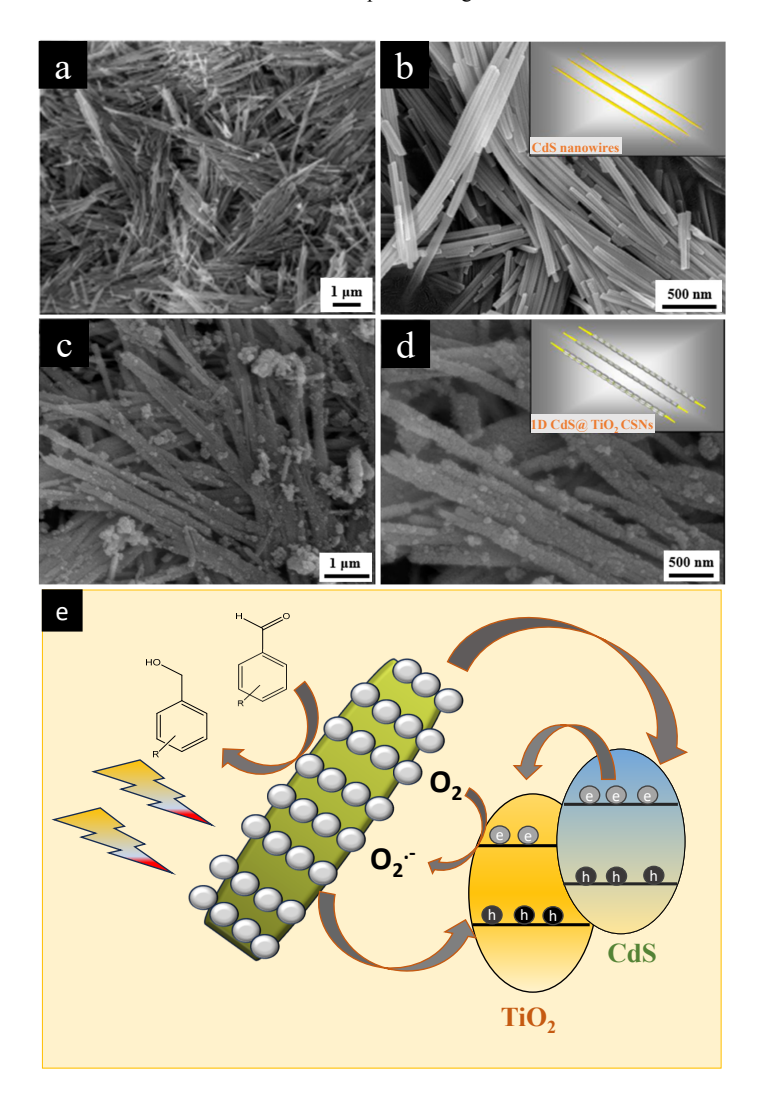


Fig. (15). SEM images of the samples of (**a**, **b**) CdS NWs and (**c**, **d**) 1D CdS@TiO₂ CSNs at different magnifications (**e**) Illustration of the proposed reaction mechanism for selective oxidation of alcohols to corresponding aldehydes over the 1D CdS@ TiO₂ CSNs under visible-light irradiation. Reprinted with permission from ref [4]. Copyright (2012), *ACS Appl. Mater. Interfaces*.

Hydrazine used in the reaction acts as the source for proton and electron and prevents the photo corrosion of CdS. The quantum confinement effect of CdS flowers leads to higher interfacial charge transfer. It provides a large surface area and provides more channels for electron transfer, which ultimately results in higher efficiency [85].

Core-shell structures with compatible band gaps prove to provide enhanced physical and chemical properties [4, 39, 86]. A combination of 1D structures with core-shell structures exhibits unique optical and electronic properties. This can be attributed to the larger specific surface area, pore volume, and high length-to-diameter ratio, along with faster and longdistance electron transport of 1D nanostructures. Based on the benefits associated with the use of core-shell nanostructures, CdS-TiO₂ core-shell nanocomposite was used for the very first time for selective alcohol oxidation and reduction of Cr (VI) reaction. The dense coat of TiO2 over the surface of CdS

nanowires with (101) exposed planes (Fig. 15) not only helped with the suppression of electron-hole recombination but also prevented the holes photogenerated in the CdS core from tunneling to the TiO2 shell. This synergic effect of such a combination resulted in better conversion as compared to bare CdS nanowires [4].

Fig. (16) shows a CdS@CdTe@MoS₂ core-shell heterostructure formed by the self-transformation of CdS nanowires to CdTe, which is subsequently enclosed within an ultrathin shell of MoS₂. This unique dual core-shell structure helps with the smooth transfer of electrons from CdTe to the outermost MoS₂ shell, thus passivating the effects of CdTe. Such photocatalysts with a unique morphology showed excellent photocatalytic activity for solar hydrogen evolution [29]. However, the effect of such control over the morphology of metal-chalcogenide-based heterostructures is still underexplored for organic transformation.

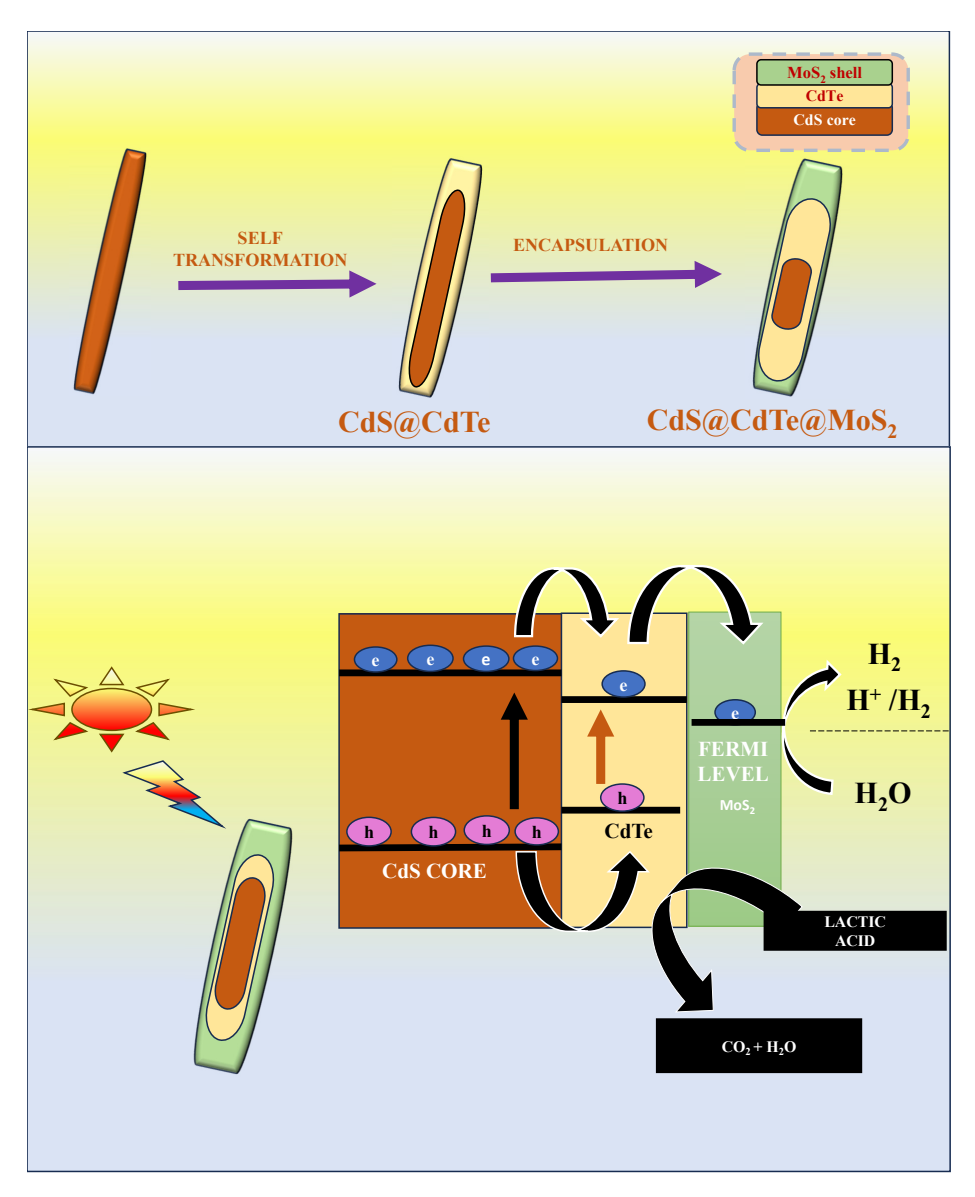


Fig. (16). Proposed Photocatalytic Mechanism of CdS@CdTe@MoS2 Dual Core-Shell Ternary Heterostructure.

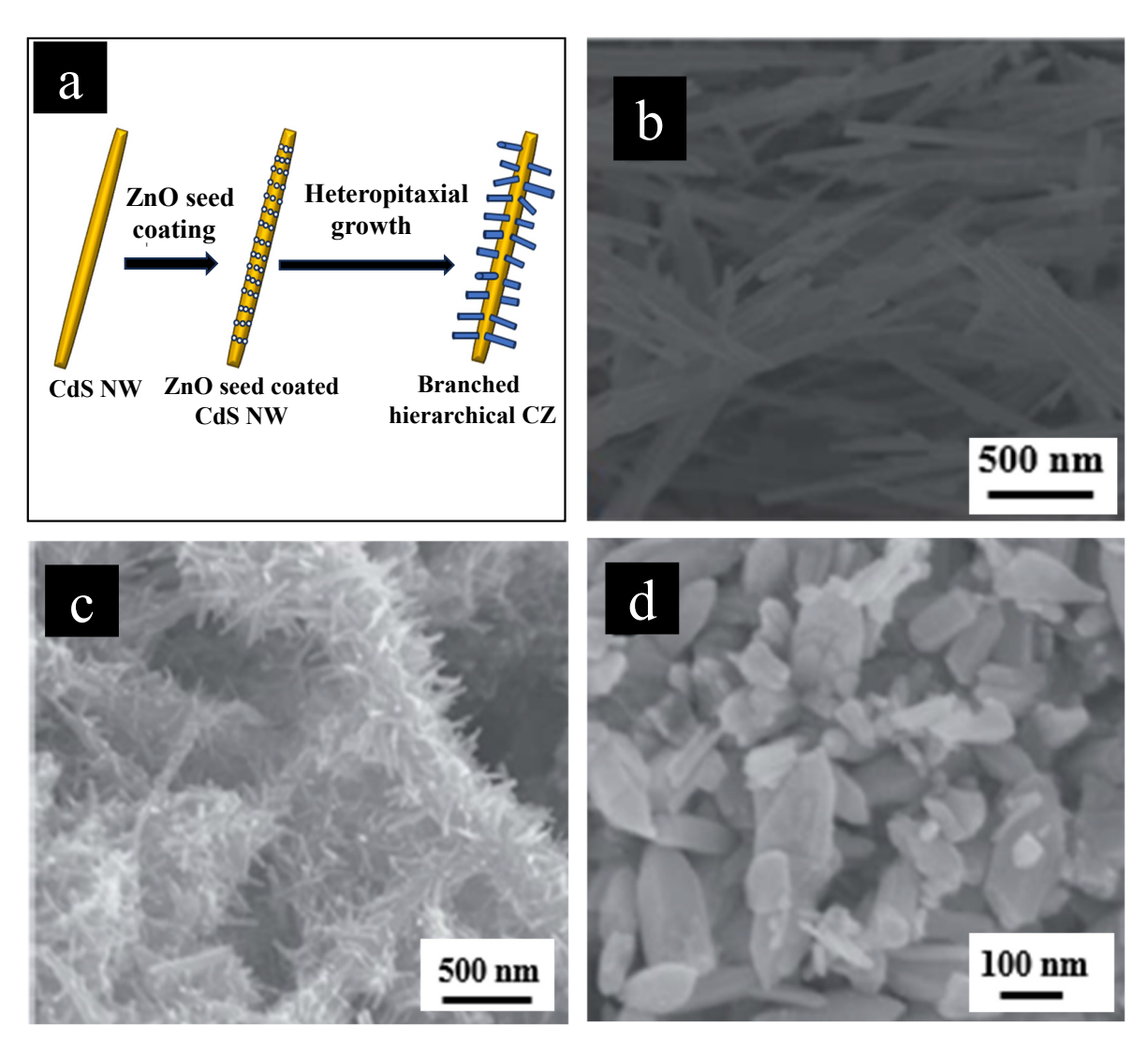


Fig. (17). A schematic demonstration of of synthesis of branched hierarchical CZ nanocomposites (a); SEM images of CdS NWs (b), branched hierarchical CZ nanocomposites (c), and blank ZnO (d). Reprinted with permission from ref [87]. Copyright (2014), *Nanoscale*.

Keeping in view the photoharvesting advantages associated with hollow structure with porous shell, a novel In $_2$ O $_3$ -In $_2$ S $_3$ heterostructure modified by N-doped carbon having a hierarchical hollow dodecahedral morphology (In $_2$ O $_3$ -In $_2$ S $_3$ /N-C HDS) was also developed which proved to improve charge separation and enhance light absorption abilities by causing multiple reflections in its hollow internal cavity [26].

Similarly, hierarchical nanostructures with different 1D cores and branches prove to provide excellent photocatalytic activity due to reduced reflection and multi-scattering (Fig. 17). To make utmost benefit of such hierarchical structure, a nano tree-like CdS/ZnO hierarchical nanostructures was developed for photocatalytic aerobic selective sulfoxidation and anaerobic reduction of 4-nitroaniline. Their developed photocatalyst exhibited better photocatalytic activity than both ZnO nanorods and CdS nanowires. This is due to the fact that the formation of such hierarchical heterostructures actually passivates the surface defects and hence can boost charge carrier transport [88].

The Hierarchical nanosheet-assembled hollow cubic architecture have shown tremendous potential for photocatalytic oxidative transformations as compared to smooth surfaces because of better light absorption ability along with more catalytically active sites [88].

2D/2D heterostructures possess tremendous face-to-face contact, resulting in upliftment in charge mobility across the hetero surfaces, thus preventing charge recombination and consequently resulting in better photocatalytic activity. pH of the medium combined with the other properties of photocatalyst plays a crucial role in deciding the products of the organic synthesis. Photocatalytic biomass conversions of furfural and 5-Hydroxymethylfurfural (HMF) are found to require an alkaline medium to yield furoic acid and 2,5-Furandicarboxykic acid (FDCA) with excellent selectivity (Scheme 11). This uplifted selectivity is attributed to the Cannizaro reaction, which takes place only in an alkaline medium. Due to the low stability of aldehydes at high pH, they undergo disproportionation to yield alcohols and carboxylates with 90% yield [89].

Scheme (11). An illustration for photocatalytic oxidative conversions of furfural alcohol and 5-hydroxymethylfurufural catalyzed by Ni/CdS nanosheets.

Some of the organic reactions catalyzed by metal chalcogenides and their heterostructures need both light irradiation and slightly higher temperatures to proceed efficiently. It has been observed that thermal oxidation of amines yields only 27% of N-Benzylidene benzylamine, and purely photocatalytic conditions also yield less than photothermal conditions. This work emphasizes the fact that a perfect balance of both thermal and light irradiation is essential for driving the aerobic oxidation of amines efficiently when Au-Pt/Cu₂S₄-Cu₉S₈ is used for catalyzing the reaction. So, more chalcogenide-based heterostructures with tunable bandgap structures need to be developed to perform such reactions purely photocatalytically [88]. Reduced graphene oxide exhibits a "local thermal effect" near the interface, which causes absorption of superfluous electrons and, consequently, leads to joule heating, which enhances the rate of photocatalytic reactions. Thus, a composite of CdS with reduced graphene oxide seems to be an excellent photocatalyst that can easily overcome the problem of charge recombination [90].

CONCLUSION

2,5-Furandicarboxylic acid

Metal chalcogenides, with their unique electronic and optical properties, seem to be an excellently studied photocatalytic material for numerous reactions ranging from the activation of small molecules to degradation processes. However, a better understanding of mechanisms is required for its applications in photocatalytic organic transformations. The narrow optical bandgap of metal chalcogenide, low toxicity, and biocompatibility make the metal chalcogenides a better photocatalytic material, but high charge recombination, lower stability, and lesser number of catalytically active sites restricts its efficiency. To overcome the shortcomings of bare metal chalcogenides, they were combined with other materials like metal oxides, metal nanoparticles, g-C₃N₄, MOF, and many more, which proved to successfully outperform pure metal chalcogenides by exhibiting a synergistic effect. The combination of metal oxide and chalcogenide nanoparticles in heterostructures provides a versatile and efficient platform for harnessing light energy to drive photocatalytic reactions with applications ranging from environmental remediation to energy conversion. Mediators fulfilled various functions like control over the morphology, bridging of the two nanostructures, and enhancement of the transfer of charges between the two semiconductors in the creation of heterostructure photocatalysts based on chalcogenides. Materials like g-C₃N₄, MOF, TNT, and SACs are new-age photocatalytic materials that, when combined with metal chalcogenides, form heterostructures, which can exhibit unmatched catalytic efficiency and selectivity for organic transformations. Different morphologies of nanostructures expose different planes and defects owing to different mechanisms and pathways for electron flow. Moreover, the size of nanostructures also influences the quantum confinement effect, which is extremely crucial for the narrowing of the bandgap. It has been observed that industrially important organic transformations are usually not sustainable because of the adverse reaction conditions they require, such as high temperature and pressure. Considering the status of research on metal chalcogenide-based heterostructures, it can be concluded that chalcogenide is an immensely potent and versatile semiconductor whose properties and stability can be enhanced by exhibiting synergistic effects with other materials. However, a poor understanding of the catalytic surfaces and metal-substrate interaction is restricting its applications to only a few of the reactions. more morphology-controlled chalcogenide-based heterostructures need to be developed for organic transformations soon. Moreover, a good understanding of the surface interactions leads to a better understanding of various reaction mechanisms, which ultimately helps with the development of more selective and highly efficient photocatalysts for industrially important organic transformations, ultimately leading to a sustainable future.

LIST OF ABBREVIATIONS

NPs = Nanoparticles
NWs = Nanowires
CB = Conduction Band
VB = Valence Band

TMCs = Transition Metal Chalcogenides

MOF = Metal-organic framework

TNT = Titanate nanotubes
SACs = Single-atom catalysts
ODs = Quantum dots

CONSENT FOR PUBLICATION

Not applicable.

FUNDING

None.

CONFLICT OF INTEREST

The authors declare no conflict of interest, financial or otherwise.

ACKNOWLEDGEMENTS

Declared none.

REFERENCES

- [1] Muralirajan, K.; Kancherla, R.; Bau, J.A.; Taksande, M.R.; Qureshi, M.; Takanabe, K.; Rueping, M. Exploring the Structure and Performance of Cd-Chalcogenide Photocatalysts in Selective Trifluoromethylation. ACS Catal., 2021, 11(24), 14772-14780. [http://dx.doi.org/10.1021/acscatal.1c04053]
- [2] Naseri, M.; Bafekry, A.; Faraji, M.; Hoat, D.M.; Fadlallah, M.M.; Ghergherehchi, M.; Sabbaghi, N.; Gogova, D. Two-dimensional buckled tetragonal cadmium chalcogenides including CdS, CdSe, and CdTe monolayers as photo-catalysts for water splitting. *Phys. Chem. Chem. Phys.*, 2021, 23(21), 12226-12232. [http://dx.doi.org/10.1039/D1CP00317H] [PMID: 34009225]
- [3] Wu, X.J.; Chen, J.; Tan, C.; Zhu, Y.; Han, Y.; Zhang, H. Controlled growth of high-density CdS and CdSe nanorod arrays on selective facets of two-dimensional semiconductor nanoplates. *Nat. Chem.*, 2016, 8(5), 470-475.
 - [http://dx.doi.org/10.1038/nchem.2473] [PMID: 27102681]
- [4] Liu, S.; Zhang, N.; Tang, Z.R.; Xu, Y.J. Synthesis of one-dimensional CdS@TiO₂ core-shell nanocomposites photocatalyst for selective redox: the dual role of TiO₂ shell. ACS Appl. Mater. Interfaces, 2012, 4(11), 6378-6385. [http://dx.doi.org/10.1021/am302074p] [PMID: 23131118]
- [5] Huo, S.; Chen, C. One-step synthesis CdS/single crystal ZnO nanorod heterostructures with high photocatalytic H₂ production ability. *Inorg. Chem. Commun.*, 2021, 132, 108841. [http://dx.doi.org/10.1016/j.inoche.2021.108841]
- [6] Zhang, P.; Liu, Y.; Tian, B.; Luo, Y.; Zhang, J. Synthesis of core-shell structured CdS@CeO₂ and CdS@TiO₂ composites and comparison of their photocatalytic activities for the selective oxidation of benzyl alcohol to benzaldehyde. *Catal. Today*, 2017, 281, 181-188. [http://dx.doi.org/10.1016/j.cattod.2016.05.042]
- [7] Wang, L.; Wang, C.; Liu, W.; Chen, Q.; He, M. Visible-light-induced aerobic thiocyanation of indoles using reusable TiO2/MoS2 nanocomposite photocatalyst. *Tetrahedron Lett.*, 2016, 57(16), 1771-1774. [http://dx.doi.org/10.1016/j.tetlet.2016.03.028]
- [8] Chai, Z.; Zeng, T.T.; Li, Q.; Lu, L.Q.; Xiao, W.J.; Xu, D. Efficient visible light-driven splitting of alcohols into hydrogen and corresponding carbonyl compounds over a Ni-modified CdS photocatalyst. J. Am. Chem. Soc., 2016, 138(32), 10128-10131. [http://dx.doi.org/10.1021/jacs.6b06860] [PMID: 27477237]
- [9] Xiang, X.; Zhu, B.; Zhang, J.; Jiang, C.; Chen, T.; Yu, H.; Yu, J.; Wang, L. Photocatalytic H₂-production and benzyl-alcohol-oxidation mechanism over CdS using Co²⁺ as hole cocatalyst. *Appl. Catal. B*, 2023, 324, 122301. [http://dx.doi.org/10.1016/j.apcatb.2022.122301]
- [10] Kumar, P.S.; Lakshmi Prabavathi, S.; Indurani, P.; Karuthapandian, S.; Muthuraj, V. Light assisted synthesis of hierarchically structured Cu/CdS nanorods with superior photocatalytic activity, stability and photocatalytic mechanism. Separ. Purif. Tech., 2017, 172, 192-201. [http://dx.doi.org/10.1016/j.seppur.2016.08.017]
- [11] Zhang, N.; Liu, S.; Fu, X.; Xu, Y.J. Fabrication of coenocytic Pd@CdS nanocomposite as a visible light photocatalyst for selective transformation under mild conditions. J. Mater. Chem., 2012, 22(11), 5042-5052.
- [http://dx.doi.org/10.1039/c2jm15009c]
- [12] Chen, L.; Xu, Y.; Chen, B. *In situ* photochemical fabrication of CdS/g-C₃N₄ nanocomposites with high performance for hydrogen evolution under visible light. *Appl. Catal. B*, **2019**, *256*, 117848. [http://dx.doi.org/10.1016/j.apcatb.2019.117848]
- [13] Vu, N.N.; Kaliaguine, S.; Do, T.O. Synthesis of the g-C₃N₄/CdS nanocomposite with a chemically bonded interface for enhanced sunlight-driven CO₂ photoreduction. ACS Appl. Energy Mater., 2020, 3(7), 6422-6433.
 - [http://dx.doi.org/10.1021/acsaem.0c00656]
- [14] Van, K.N.; Huu, H.T.; Nguyen Thi, V.N.; Thi Le, T.L.; Hoang, Q.D.; Dinh, Q.V.; Vo, V.; Tran, D.L.; Vasseghian, Y. Construction of S-scheme CdS/g-C₃N₄ nanocomposite with improved visible-light photocatalytic degradation of methylene blue. *Environ. Res.*, 2022, 206, 112556.
 - [http://dx.doi.org/10.1016/j.envres.2021.112556] [PMID: 34951992]

- [15] Yuan, C.; Liu, Q.; Wei, M.; Zhao, S.; Yang, X.; Cao, B.; Wang, S.; El-Fatah Abomohra, A.; Liu, X.; Hu, Y. Selective oxidation of 5-hydroxymethylfurfural to furan-2,5-dicarbaldehyde using chitosan-based biochar composite cadmium sulfide quantum dots. *Fuel*, 2022, 320, 123994. [http://dx.doi.org/10.1016/j.fuel.2022.123994]
- [16] Wang, X.X.; Meng, S.; Zhang, S.; Zheng, X.; Chen, S. 2D/2D MXene/g-C₃N₄ for photocatalytic selective oxidation of 5-hydroxymethylfurfural into 2,5-formylfuran. *Catal. Commun.*, 2020, 147, 106152. [http://dx.doi.org/10.1016/j.catcom.2020.106152]
- [17] Saka, C. Performance of g-C₃N₄ nanoparticles by EDTA modification and protonation for hydrogen release from sodium borohydride methanolysis. *Int. J. Hydrogen Energy*, 2022, 47(28), 13654-13663. [http://dx.doi.org/10.1016/j.ijhydene.2022.02.121]
- [18] Wang, J.; Pan, R.; Hao, Q.; Gao, Y.; Ye, J.; Wu, Y.; van Ree, T. Constructing Defect-Mediated CdS/g-C₃N₄ by an In-situ interlocking strategy for Cocatalyst-free photocatalytic H₂ production. *Appl. Surf. Sci.*, 2022, 599, 153875. [http://dx.doi.org/10.1016/j.apsusc.2022.153875]
- [19] Zheng, J.; Lebedev, K.; Wu, S.; Huang, C.; Ayvalı, T.; Wu, T.S.; Li, Y.; Ho, P.L.; Soo, Y.L.; Kirkland, A.; Tsang, S.C.E. High loading of transition metal single atoms on chalcogenide catalysts. *J. Am. Chem. Soc.*, 2021, 143(21), 7979-7990.
 [http://dx.doi.org/10.1021/jacs.1c01097] [PMID: 34019424]
- [20] Liang, R.; Jing, F.; Yan, G.; Wu, L. Synthesis of CdS-decorated MIL-68(Fe) nanocomposites: Efficient and stable visible light photocatalysts for the selective reduction of 4-nitroaniline to pphenylenediamine in water. Appl. Catal. B, 2017, 218, 452-459. [http://dx.doi.org/10.1016/j.apcatb.2017.06.075]
- [21] Navakoteswara Rao, V.; Ravi, P.; Sathish, M.; Vijayakumar, M.; Sakar, M.; Karthik, M.; Balakumar, S.; Reddy, K.R.; Shetti, N.P.; Aminabhavi, T.M.; Shankar, M.V. Metal chalcogenide-based core/shell photocatalysts for solar hydrogen production: Recent advances, properties and technology challenges. *J. Hazard. Mater.*, 2021, 415, 125588. [http://dx.doi.org/10.1016/j.jhazmat.2021.125588] [PMID: 33756202]
- [22] Ashraf, M.A.; Yang, Y.; Fakhri, A. Synthesis of NiS-MoO₃ nanocomposites and decorated on graphene oxides for heterogeneous photocatalysis, antibacterial and antioxidant activities. *Ceram. Int.*, 2020, 46(6), 8379-8384. [http://dx.doi.org/10.1016/j.ceramint.2019.12.070]
- [23] Jana, T.K.; Maji, S.K.; Pal, A.; Maiti, R.P.; Dolai, T.K.; Chatterjee, K. Photocatalytic and antibacterial activity of cadmium sulphide/zinc oxide nanocomposite with varied morphology. *J. Colloid Interface Sci.*, 2016, 480, 9-16. [http://dx.doi.org/10.1016/j.jcis.2016.06.073] [PMID: 27399614]
- [24] Balapure, A.; Ray Dutta, J.; Ganesan, R. Recent advances in semiconductor heterojunctions: a detailed review of the fundamentals of photocatalysis, charge transfer mechanism and materials. RSC Applied Interfaces, 2024, 1(1), 43-69. [http://dx.doi.org/10.1039/D3LF00126A]
- [25] Shafiee, A.; Rabiee, N.; Ahmadi, S.; Baneshi, M.; Khatami, M.; Iravani, S.; Varma, R.S. Core-shell nanophotocatalysts: review of materials and applications. ACS Appl. Nano Mater., 2022, 5(1), 55-86. [http://dx.doi.org/10.1021/acsanm.1c03714]
- [26] Shen, Q.; Sun, L.; Zhuang, Y.; Zhan, W.; Wang, X.; Han, X. Hollow dodecahedral structure of In₂O₃-In₂S₃ heterojunction encapsulated by N-doped C as an excellent visible-light-active photocatalyst for organic transformation. *Inorg. Chem.*, 2020, 59(23), 17650-17658. [http://dx.doi.org/10.1021/acs.inorgchem.0c02892] [PMID: 33206500]
- [27] Gogoi, P.; Saikia, T.; Hazarika, R.; Garg, A.; Deori, K.; Sarma, D. Ultralow-loading copper sulfide nanosheets on g-C₃ N₄ as a visible-light-active photocatalyst for the regioselective synthesis of 1,4-disubstituted 1,2,3-triazoles. ACS Sustain. Chem. Eng., 2023, 11(42), 15207-15217. [http://dx.doi.org/10.1021/acssuschemeng.3c02827]
- [28] Taghinejad, H.; Taghinejad, M.; Eftekhar, A.A.; Li, Z.; West, M.P.; Javani, M.H.; Abdollahramezani, S.; Zhang, X.; Tian, M.; Johnson-Averette, T.; Ajayan, P.M.; Vogel, E.M.; Shi, S.F.; Cai, W.; Adibi, A. Synthetic engineering of morphology and electronic band gap in lateral heterostructures of monolayer transition metal dichalcogenides. ACS Nano, 2020, 14(5), 6323-6330. [http://dx.doi.org/10.1021/acsnano.0c02885] [PMID: 32364693]
- [29] Fu, X.Y.; Li, Y.B.; Huang, M.H.; Li, T.; Dai, X.C.; Hou, S.; Wei, Z.Q.; Xiao, F.X. Partially self-transformed transition-metal

- chalcogenide interim layer: motivating charge transport cascade for solar hydrogen evolution. *Inorg. Chem.*, **2020**, *59*(4), 2562-2574. [http://dx.doi.org/10.1021/acs.inorgchem.9b03538] [PMID: 32013411]
- [30] Liu, Y.; Huang, D.; Cheng, M.; Liu, Z.; Lai, C.; Zhang, C.; Zhou, C.; Xiong, W.; Qin, L.; Shao, B.; Liang, Q. Metal sulfide/MOF-based composites as visible-light-driven photocatalysts for enhanced hydrogen production from water splitting. *Coord. Chem. Rev.*, 2020, 409, 213220.
- [31] Yang, T.; Yu, J.M.; Zhai, L.; Jia, S.; Yang, C.; Xiong, W.W.; Zhang, Q. An inorganic-organic hybrid indium tin selenide featuring a two-dimensional layered structure for high efficient photocatalytic Cr(VI) reduction. J. Clean. Prod., 2023, 414, 137643.

[http://dx.doi.org/10.1016/j.ccr.2020.213220]

- [http://dx.doi.org/10.1016/j.jclepro.2023.137643]
 [32] Madkour, M.; Abdelmonem, Y.; Qazi, U.Y.; Javaid, R.; Vadivel, S. Efficient Cr(VI) photoreduction under natural solar irradiation using a novel step-scheme ZnS/SnIn 4 S 8 nanoheterostructured photocatalysts. RSC Advances, 2021, 11(47), 29433-29440.
 [http://dx.doi.org/10.1039/D1RA04649G] [PMID: 35492066]
- [33] Tan, Y.X.; Chai, Z.M.; Wang, B.H.; Tian, S.; Deng, X.X.; Bai, Z.J.; Chen, L.; Shen, S.; Guo, J.K.; Cai, M.Q.; Au, C.T.; Yin, S.F. Boosted photocatalytic oxidation of toluene into benzaldehyde on CdIn₂S₄-CdS: Synergetic effect of compact heterojunction and S-vacancy. ACS Catal., 2021, 11(5), 2492-2503. [http://dx.doi.org/10.1021/acscatal.0c05703]
- [34] Agarwal, S.; Deori, K. Copper sulfide nanosheets for photocatalytic oxidation of benzyl alcohols and hydroxylation of arylboronic acids. ACS Appl. Nano Mater., 2022, 5(3), 4413-4422. [http://dx.doi.org/10.1021/acsanm.2c00516]
- [35] Zhou, M.; Xiao, K.; Jiang, X.; Huang, H.; Lin, Z.; Yao, J.; Wu, Y. Visible-light-responsive chalcogenide photocatalyst Ba2ZnSe3: crystal and electronic structure, thermal, optical, and photocatalytic activity. *Inorg. Chem.*, 2016, 55(24), 12783-12790.
 [http://dx.doi.org/10.1021/acs.inorgchem.6b02072] [PMID: 27989175]
- [36] Li, B.; Wang, Y. Synthesis, microstructure, and photocatalysis of ZnO/CdS nano-heterostructure. J. Phys. Chem. Solids, 2011, 72(10), 1165-1169. [http://dx.doi.org/10.1016/j.jpcs.2011.07.010]
- [37] Eidsvåg, H.; Bentouba, S.; Vajeeston, P.; Yohi, S.; Velauthapillai, D. TiO₂ as a photocatalyst for water splitting—An experimental and theoretical review. *Molecules*, 2021, 26(6), 1687. [http://dx.doi.org/10.3390/molecules26061687] [PMID: 33802911]
- [38] Zhang, Y.; Xu, X. Machine learning band gaps of doped-TiO₂ photocatalysts from structural and morphological parameters. ACS Omega, 2020, 5(25), 15344-15352. [http://dx.doi.org/10.1021/acsomega.0c01438] [PMID: 32637808]
- [39] Armaković, S.J.; Savanović, M.M.; Armaković, S. Titanium dioxide as the most used photocatalyst for water purification: An overview. *Catalysts*, 2022, 13(1), 26. [http://dx.doi.org/10.3390/catal13010026]
- [40] Adabala, S.; Dutta, D.P. A review on recent advances in metal chalcogenide-based photocatalysts for CO₂ reduction. *J. Environ. Chem. Eng.*, 2022, 10(3), 107763. [http://dx.doi.org/10.1016/j.jece.2022.107763]
- [41] Guo, X.; Chen, C.; Song, W.; Wang, X.; Di, W.; Qin, W. CdS embedded TiO₂ hybrid nanospheres for visible light photocatalysis. *J. Mol. Catal. Chem.*, 2014, 387, 1-6. [http://dx.doi.org/10.1016/j.molcata.2014.02.020]
- [42] Maurya, A.; Chauhan, P. Structural and optical characterization of CdS/TiO₂ nanocomposite. *Mater. Charact.*, 2011, 62(4), 382-390. [http://dx.doi.org/10.1016/j.matchar.2011.01.014]
- [43] Lee, S.Y.; Park, S.J. TiO₂ photocatalyst for water treatment applications. J. Ind. Eng. Chem., 2013, 19(6), 1761-1769. [http://dx.doi.org/10.1016/j.jiec.2013.07.012]
- [44] Banerjee, S.; Mohapatra, S.K.; Das, P.P.; Misra, M. Synthesis of coupled semiconductor by filling 1D TiO₂ nanotubes with CdS. *Chem. Mater.*, 2008, 20(21), 6784-6791. [http://dx.doi.org/10.1021/cm802282t]
- [45] Xie, Y.; Ali, G.; Yoo, S.H.; Cho, S.O. Sonication-assisted synthesis of CdS quantum-dot-sensitized TiO₂ nanotube arrays with enhanced photoelectrochemical and photocatalytic activity. ACS Appl. Mater. Interfaces, 2010, 2(10), 2910-2914. [http://dx.doi.org/10.1021/am100605a] [PMID: 20849087]
- [46] Tamiolakis, I.; Lykakis, I.N.; Armatas, G.S. Mesoporous CdS-sensitized TiO₂ nanoparticle assemblies with enhanced photocatalytic properties: Selective aerobic oxidation of benzyl alcohols. *Catal.*

- *Today*, **2015**, *250*, 180-186. [http://dx.doi.org/10.1016/j.cattod.2014.03.047]
- [47] Widiyandari, H.; Ketut Umiati, N.A.; Dwi Herdianti, R. Synthesis and photocatalytic property of Zinc Oxide (ZnO) fine particle using flame spray pyrolysis method. J. Phys. Conf. Ser., 2018, 1025, 012004. [http://dx.doi.org/10.1088/1742-6596/1025/1/012004]
- [48] Raza, W.; Faisal, S.M.; Owais, M.; Bahnemann, D.; Muneer, M. Facile fabrication of highly efficient modified ZnO photocatalyst with enhanced photocatalytic, antibacterial and anticancer activity. RSC Advances, 2016, 6(82), 78335-78350. [http://dx.doi.org/10.1039/C6RA06774C]
- [49] Hanafi, M.F.; Sapawe, N. An overview of recent developments on semiconductor catalyst synthesis and modification used in photocatalytic reaction. *Mater. Today*, 2020, 31, A151-A157.
- [50] Wang, S.; Zhu, B.; Liu, M.; Zhang, L.; Yu, J.; Zhou, M. Direct Z-scheme ZnO/CdS hierarchical photocatalyst for enhanced photocatalytic H₂-production activity. *Appl. Catal. B*, 2019, 243, 19-26. [http://dx.doi.org/10.1016/j.apcatb.2018.10.019]
- [51] Kundu, P.; Deshpande, P.A.; Madras, G.; Ravishankar, N. Nanoscale ZnO/CdS heterostructures with engineered interfaces for high photocatalytic activity under solar radiation. J. Mater. Chem. A Mater. Energy Sustain.. 2011. 21, 4209-4216.
- [52] Tran, D.P.H.; Pham, M.T.; Bui, X.T.; Wang, Y.F.; You, S.J. CeO₂ as a photocatalytic material for CO₂ conversion: A review. *Sol. Energy*, 2022, 240, 443-466. [http://dx.doi.org/10.1016/j.solener.2022.04.051]
- [53] Zhang, X.; Zhang, N.; Xu, Y.J.; Tang, Z.R. One-dimensional CdS nanowires—CeO₂ nanoparticles composites with boosted photocatalytic activity. New J. Chem., 2015, 39(9), 6756-6764. [http://dx.doi.org/10.1039/C5NJ00976F]
- [54] Mou, Q.; Guo, Z.; Chai, Y.; Liu, B.; Liu, C. Visible light assisted production of methanol from CO₂ using CdS@CeO₂ heterojunction. *J. Photochem. Photobiol. B*, 2021, 219, 112205. [http://dx.doi.org/10.1016/j.jphotobiol.2021.112205] [PMID: 33957468]
- [55] Li, Z.; Meng, X.; Zhang, Z. Recent development on MoS2-based photocatalysis: A review. J. Photochem. Photobiol. Photochem. Rev., 2018, 35, 39-55. [http://dx.doi.org/10.1016/j.jphotochemrev.2017.12.002]
- [56] Sivaranjani, P.R.; Janani, B.; Thomas, A.M.; Raju, L.L.; Khan, S.S. Recent development in MoS2-based nano-photocatalyst for the degradation of pharmaceutically active compounds. *J. Clean. Prod.*, 2022, 352, 131506. [http://dx.doi.org/10.1016/j.jclepro.2022.131506]
- [57] Liu, W.; Wang, C.; Huang, Y.; Chen, Q.; Wang, L.; He, M. Visible-light-mediated facile synthesis of disulfides using reusable TiO₂/MoS₂ nanocomposite photocatalyst. *Synth. Commun.*, 2016, 46(15), 1268-1274. [http://dx.doi.org/10.1080/00397911.2016.1199808]
- [58] Yang, H.; Jin, Z.; Fan, K.; Liu, D.; Lu, G. The roles of Ni nanoparticles over CdS nanorods for improved photocatalytic stability and activity. *Superlattices Microstruct.*, 2017, 111, 687-695. [http://dx.doi.org/10.1016/j.spmi.2017.07.025]
- [59] Luo, M.; Liu, Y.; Hu, J.; Liu, H.; Li, J. One-pot synthesis of CdS and Ni-doped CdS hollow spheres with enhanced photocatalytic activity and durability. ACS Appl. Mater. Interfaces, 2012, 4(3), 1813-1821. [http://dx.doi.org/10.1021/am3000903] [PMID: 22387732]
- [60] Wang, W.; Li, T.; Komarneni, S.; Lu, X.; Liu, B. Recent advances in Co-based co-catalysts for efficient photocatalytic hydrogen generation. J. Colloid Interface Sci., 2022, 608(Pt 2), 1553-1575. [http://dx.doi.org/10.1016/j.jcis.2021.10.051] [PMID: 34742073]
- [61] Yang, X.; Wang, Z.; Lv, X.; Wang, Y.; Jia, H. Enhanced photocatalytic activity of Zn-doped dendritic-like CdS structures synthesized by hydrothermal synthesis. J. Photochem. Photobiol. Chem., 2016, 329, 175-181. [http://dx.doi.org/10.1016/j.jphotochem.2016.07.005]
- [62] Mitkina, T.; Stanglmair, C.; Setzer, W.; Gruber, M.; Kisch, H.; König, B. Visible light mediated homo- and heterocoupling of benzyl alcohols and benzyl amines on polycrystalline cadmium sulfide. *Org. Biomol. Chem.*, 2012, 10(17), 3556-3561. [http://dx.doi.org/10.1039/c2ob07053g] [PMID: 22447128]
- [63] Yu, W.; Zhang, D.; Guo, X.; Song, C.; Zhao, Z. Enhanced visible light photocatalytic non-oxygen coupling of amines to imines integrated with hydrogen production over Ni/CdS nanoparticles. *Catal. Sci. Technol.*, 2018, 8(20), 5148-5154.

- [http://dx.doi.org/10.1039/C8CY01326H]
- [64] Iqbal, M.; Ibrar, A.; Ali, A.; Rehman, F.; Jatoi, A.H.; Jatoi, W.B.; Phulpoto, S.N.; Thebo, K.H. Facile synthesis of Zn-doped CdS nanowires with efficient photocatalytic performance. *Environ. Technol.*, 2022, 43(12), 1783-1790. [http://dx.doi.org/10.1080/09593330.2020.1850880] [PMID: 33180681]
- [65] Lin, X.; Xu, S.; Wei, Z.Q.; Hou, S.; Mo, Q.L.; Fu, X.Y.; Xiao, F.X. Selective organic transformation over a self-assembled all-solid-state Z-scheme core–shell photoredox system. J. Mater. Chem. A Mater. Energy Sustain., 2020, 8(38), 20151-20161. [http://dx.doi.org/10.1039/D0TA07235D]
- [66] Zhang, N.; Liu, S.; Xu, Y.J. Recent progress on metal core@semiconductor shell nanocomposites as a promising type of photocatalyst. *Nanoscale*, 2012, 4(7), 2227-2238. [http://dx.doi.org/10.1039/c2nr00009a] [PMID: 22362188]
- [67] Liu, S.; Zhang, N.; Xu, Y.J. Core–shell structured nanocomposites for photocatalytic selective organic transformations. *Part. Part. Syst. Charact.*, 2014, 31(5), 540-556. [http://dx.doi.org/10.1002/ppsc.201300235]
- [68] Higashimoto, S.; Kitao, N.; Yoshida, N.; Sakura, T.; Azuma, M.; Ohue, H.; Sakata, Y. Selective photocatalytic oxidation of benzyl alcohol and its derivatives into corresponding aldehydes by molecular oxygen on titanium dioxide under visible light irradiation. *J. Catal.*, 2009, 266(2), 279-285. [http://dx.doi.org/10.1016/j.jcat.2009.06.018]
- [69] Wu, H.; Meng, S.; Zhang, J.; Zheng, X.; Wang, Y.; Chen, S.; Qi, G.; Fu, X. Construction of two-dimensionally relative p-n heterojunction for efficient photocatalytic redox reactions under visible light. *Appl. Surf. Sci.*, 2020, 505, 144638. [http://dx.doi.org/10.1016/j.apsusc.2019.144638]
- [70] Ye, X.; Dai, X.; Meng, S.; Fu, X.; Chen, S. A Novel CDS /g□ C, N, Composite Photocatalyst: Preparation, Characterization and Photocatalytic Performance with Different Reaction Solvents under Visible Light Irradiation. Chin. J. Chem., 2017, 35(2), 217-225. [http://dx.doi.org/10.1002/cjoc.201600251]
- [71] Wang, Z.; Lu, D.; Pan, J.; Kumar Kondamareddy, K.; Gu, W.; Li, J.; Zhang, B.; Wu, J.; Fan, H.; Ho, W. Efficient photocatalytic dehydrogenation and synergistic selective oxidation of benzyl alcohol to benzaldehyde for Zn0.5Cd0.5S co-modified with MoS₂ nanoflowers and g-C₃N₄ nanosheets. *Appl. Surf. Sci.*, **2023**, *640*, 158384. [http://dx.doi.org/10.1016/j.apsusc.2023.158384]
- [72] Tian, S.; Yang, Q.; Zheng, W.; Yang, A. CdS decorated graphitic carbon nitride catalyzed one-pot hydrogenation of nitroaromatics and benzylamine derivatives coupling under visible light irradiation. *Fuel*, 2023, 334, 126586. [http://dx.doi.org/10.1016/j.fuel.2022.126586]
- [73] He, J.; Chen, L.; Ding, D.; Yang, Y.K.; Au, C.T.; Yin, S.F. Facile fabrication of novel Cd₃(C₃N₃S₃)₂/CdS porous composites and their photocatalytic performance for toluene selective oxidation under visible light irradiation. *Appl. Catal. B*, 2018, 233, 243-249. [http://dx.doi.org/10.1016/j.apcatb.2018.04.008]
- [74] Tang, Z.R.; Yin, X.; Zhang, Y.; Xu, Y.J. Synthesis of titanate nanotube-CdS nanocomposites with enhanced visible light photocatalytic activity. *Inorg. Chem.*, **2013**, *52*(20), 11758-11766. [http://dx.doi.org/10.1021/ic4010483] [PMID: 24074302]
- [75] Xiao, M.; Wang, L.; Wu, Y.; Huang, X.; Dang, Z. Preparation and characterization of CdS nanoparticles decorated into titanate nanotubes and their photocatalytic properties. *Nanotechnology*, 2008, 19(1), 015706.
 [http://dx.doi.org/10.1088/0957-4484/19/01/015706] [PMID: 21730547]
- [76] Long, L.; Yu, X.; Wu, L.; Li, J.; Li, X. Nano-CdS confined within titanate nanotubes for efficient photocatalytic hydrogen production under visible light illumination. *Nanotechnology*, 2014, 25(3), 035603. [http://dx.doi.org/10.1088/0957-4484/25/3/035603] [PMID: 243565341]
- [77] Wang, Q.; Zhang, D.; Chen, Y.; Fu, W.F.; Lv, X.J. Single-atom catalysts for photocatalytic reactions. ACS Sustain. Chem. Eng., 2019, 7(7), 6430-6443.
 [http://dx.doi.org/10.1021/acssuschemeng.8b06273]
- [78] Gao, C.; Low, J.; Long, R.; Kong, T.; Zhu, J.; Xiong, Y. Heterogeneous Single-atom photocatalysts: fundamentals and applications. *Chem. Rev.*, 2020, 120(21), 12175-12216. [http://dx.doi.org/10.1021/acs.chemrev.9b00840] [PMID: 32186373]
- [79] DiMeglio, J.L.; Breuhaus-Alvarez, A.G.; Li, S.; Bartlett, B.M. Nitratemediated alcohol oxidation on cadmium sulfide photocatalysts. ACS

- Catal., **2019**, *9*(6), 5732-5741. [http://dx.doi.org/10.1021/acscatal.9b01051]
- [80] Xiao, Y.; Wang, T.; Qiu, G.; Zhang, K.; Xue, C.; Li, B. Synthesis of EDTA-bridged CdS/g-C₃N₄ heterostructure photocatalyst with enhanced performance for photoredox reactions. *J. Colloid Interface* Sci., 2020, 577, 459-470. [http://dx.doi.org/10.1016/j.jcis.2020.05.099] [PMID: 32505006]
- [81] Liu, B.J.; Liang, H.; Mo, Q.L.; Li, S.; Tang, B.; Zhu, S.C.; Xiao, F.X. Unleashing non-conjugated polymers as charge relay mediators. *Chem. Sci. (Camb.)*, 2022, 13(2), 497-509. [http://dx.doi.org/10.1039/D1SC04877E] [PMID: 35126982]
- [82] Zhang, Y.; Xu, X. Predictions of glass transition onset temperature of chalcogenide glass Ge Se1-. J. Phys. Chem. Solids, 2021, 159, 110246. [http://dx.doi.org/10.1016/j.jpcs.2021.110246]
- [83] Zhang, Y.; Zhang, N.; Tang, Z.R.; Xu, Y.J. Transforming CdS into an efficient visible light photocatalyst for selective oxidation of saturated primary C–H bonds under ambient conditions. *Chem. Sci. (Camb.)*, 2012, 3(9), 2812-2822. [http://dx.doi.org/10.1039/c2sc20603j]
- [84] Chai, Z.M.; Wang, B.H.; Tan, Y.X.; Bai, Z.J.; Pan, J.B.; Chen, L.; Shen, S.; Guo, J.K.; Xie, T.L.; Au, C.T.; Yin, S.F. Enhanced photocatalytic activity for selective oxidation of toluene over cubic–hexagonal cds phase junctions. *Ind. Eng. Chem. Res.*, 2021, 60(30), 11106-11116. [http://dx.doi.org/10.1021/acs.iecr.1c01505]

- [85] Pahari, S.K.; Pal, P.; Srivastava, D.N.; Ghosh, S.C.; Panda, A.B. Efficient photocatalytic selective nitro-reduction and C-H bond oxidation over ultrathin sheet mediated CdS flowers. *Chem. Commun. (Camb.)*, 2015, 51(51), 10322-10325. [http://dx.doi.org/10.1039/C5CC01685A] [PMID: 26024214]
- [86] Sun, C.; Gu, Y.; Wen, W.; Zhao, L. ZnSe based semiconductor coreshell structures: From preparation to application. *Opt. Mater.*, 2018, 81, 12-22.
 - [http://dx.doi.org/10.1016/j.optmat.2018.05.005]
- [87] Liu, S.; Yang, M.Q.; Tang, Z.R.; Xu, Y.J. A nanotree-like CdS/ZnO nanocomposite with spatially branched hierarchical structure for photocatalytic fine-chemical synthesis. *Nanoscale*, 2014, 6(13), 7193-7198.
 [http://dx.doi.org/10.1039/c4nr01227e] [PMID: 24853606]
- [88] Gao, H.; Chen, Y.; Li, H.; Zhang, F.; Tian, G. Hierarchical Cu,S₄-Cu,S₃ heterostructure hollow cubes for photothermal aerobic oxidation of amines. Chem. Eng. J., 2019, 363, 247-258. [http://dx.doi.org/10.1016/j.cej.2019.01.137]
- [89] Wu, X.; Xie, S.; Zhang, H.; Zhang, Q.; Sels, B.F.; Wang, Y. Metal sulfide photocatalysts for lignocellulose valorization. *Adv. Mater.*, 2021, 33(50), 2007129. [http://dx.doi.org/10.1002/adma.202007129] [PMID: 34117812]
- [90] Li, Q.; Li, X.; Wageh, S.; Al-Ghamdi, A.A.; Yu, J. CdS/graphene nanocomposite photocatalysts. Adv. Energy Mater., 2015, 5(14), 1500010. [http://dx.doi.org/10.1002/aenm.201500010]

© 2024 The Author(s). Published by Bentham Science Publisher.



This is an open access article distributed under the terms of the Creative Commons Attribution 4.0 International Public License (CC-BY 4.0), a copy of which is available at: https://creativecommons.org/licenses/by/4.0/legalcode. This license permits unrestricted use, distribution, and reproduction in any medium, provided the original author and source are credited.